Defence Research and Development Canada
Recherche et développement pour la défense Canada

DEFENCE R&D DÉFENSE

On the feasibility of using measured sea clutter continuum in HFSWR to validate modelled ground-wave propagation attenuation in rough sea

Hank Leong

Defence R&D Canada – Ottawa

Technical Report
DRDC Ottawa TR 2012-015
September 2012

Canada

On the feasibility of using measured sea clutter continuum in HFSWR to validate modelled ground-wave propagation attenuation in rough sea

Hank Leong
DRDC Ottawa

Defence R&D Canada – Ottawa

Technical Report
DRDC Ottawa TR 2012-015
September 2012

Principal Author

Original signed by Hank Leong

Hank Leong

Defence Scientist

Approved by

Original signed by Anthony Damini

Anthony Damini

Acting Section Head/Radar Systems

Approved for release by

Original signed by Chris McMillan

Chris McMillan

Chief Scientist

Abstract

This report presents the results of an investigation on the feasibility of using the sea clutter continuum between the Bragg lines of monostatic HF Surface Wave Radar (HFSWR) to validate the ground-wave propagation attenuation model for rough sea, based on Barrick's formulation. The proposed validation is based on a comparison between the measured and modelled sea clutter levels from a variety of sea states over a range interval approximately between 63 and 200 km. The sea state in the interval was roughly indicated by the significant wave height measured at the far side of the radar coverage. The measured sea clutter is estimated from the median of the averaged power levels between the Bragg lines over a selected number of radar dwells in a moving window. The modelled sea clutter attenuation is then obtained by calibrating the modelled ground-wave propagation attenuation to the median sea clutter from a selected range bin in the near side of the chosen interval. The steadiness of the sea state in the selected range bin was closely monitored by the variation of the median from that range. If this median is deemed to be steady over the duration of the moving window, then the radar data segment is chosen for the investigation. The results show that the measured and modelled sea clutter attenuations agree well over the chosen interval in four different sea states at two radar frequencies. The validation is also compared with that using a dedicated ship target. It is found that the median sea echo was actually more stable than the target signal for the validation. Furthermore, the modelled sea clutter attenuation is shown to be highly sensitive to the presence of either ionospheric clutter or skywave interference. With a reasonable assumption that the sea state over the propagation path is constant, the modelled sea clutter attenuation after the validation can be used in high confidence to detect the skywave signal components.

Résumé

Le présent rapport porte sur les résultats d'une étude sur la possibilité d'utiliser le continuum de clutter de mer entre les lignes de Bragg du radar haute fréquence à ondes de surface (HFSWR) monostatique pour valider le modèle d'affaiblissement de propagation des ondes de sol en mer agitée, fondé sur la formulation de Barrick. La validation proposée repose sur une comparaison entre les niveaux de clutter de mer mesurés et modélisés à partir de divers états de la mer sur un intervalle de distances approximatif entre 63 et 200 km. L'état de mer dans l'intervalle est approximativement indiqué par la hauteur significative des vagues mesurée à l'extrémité de la couverture radar. Le clutter de mer mesuré est évalué à partir de la médiane des niveaux de puissance moyens entre les lignes de Bragg sur un nombre déterminé de temps de tenue du radar dans une fenêtre mobile. L'affaiblissement modélisé du clutter de mer est ensuite obtenu en étalonnant l'affaiblissement de propagation des ondes de sol modélisé par rapport au clutter de mer médian à partir d'une cellule de distance sélectionnée à proximité de l'intervalle choisi. La régularité de l'état de mer dans la cellule de distance sélectionnée est surveillée étroitement par la variation de la médiane à partir de cette distance. Si cette médiane est jugée régulière pendant la durée de la fenêtre mobile, le segment de données radar est alors choisi pour l'étude. Selon les résultats, les affaiblissements du clutter de mer mesurés et modélisés concordent bien sur l'intervalle choisi dans quatre états de mer distincts à deux fréquences radar. La validation est aussi comparée à celle faite à l'aide d'un navire-cible dédié. Pour la validation, on a trouvé que l'écho de mer médian est en fait plus stable que le signal de la cible. De plus, l'affaiblissement du clutter de mer modélisé s'est avéré très sensible à la présence soit de clutter ionosphérique, soit de brouillage par onde ionosphérique. En supposant de manière raisonnable que l'état de mer sur le trajet de propagation est constant, on peut utiliser sans se tromper l'affaiblissement du clutter de mer modélisé après la validation pour détecter les composantes du signal d'onde ionosphérique.

Executive summary

On the feasibility of using measured sea clutter continuum in HFSWR to validate modelled ground-wave propagation attenuation in rough sea

Hank Leong; DRDC Ottawa TR 2012-015; Defence R&D Canada – Ottawa September 2012.

Background: Modelling of HF ground-wave propagation attenuation over a rough sea makes use of Barrick's theory and the Grwave program. An attempt to validate Barrick's theory and Grwave was reported by Larson and Pielou of GEC Marconi, the same company that developed Grwave. By directly measuring the losses over a 164-km clear sea path off the coast of southwest England over a period of fourteen months, Larson and Pielou showed that the modelled propagation and observed path losses agreed well over the frequency range from 5.6 to 22.8 MHz in a variety of sea states. Here, we investigate whether it is feasible to use the sea clutter continuum between the Bragg lines of a monostatic HF Surface Wave Radar (HFSWR) system to validate the modelled ground-wave propagation attenuation in the lower portions of the HF band (3-5 MHz).

The ground-wave sea echo dominates over background noise at ranges up to 200 km. However, the sea echo may also be corrupted by ionospheric clutter and external interference. Hence, it is required to search for sets of measured HFSWR data that are not contaminated with the skywave signal components. The received power of the sea echo varies with sea state as well as ground-wave propagation attenuation. However, for a given sea state, the median of the average sea clutter between the Bragg lines is found to be fairly constant at a given range and fairly monotonic across range. For a given sea state, it is hypothesised that the sea scattering coefficient is statistically constant. With the further hypothesis that, for a fully developed sea, the sea state along the ranges in a given direction is constant, it is possible to use the measured attenuation of the ground-wave sea echo to statistically validate the modelled propagation attenuation.

Results: Sets of nighttime HFSWR data measured at the radar frequencies of 3.1 and 4.1 MHz in a variety of sea states were chosen to test the feasibility of the proposed validation. In each sea state, the median of the clutter powers between the Bragg lines along a fixed beam over a selected number of consecutive dwells is taken as a function of range. The modelled propagation attenuation for the selected sea state is scaled to the measured clutter power at a chosen range (R_0) where the sea echo is dominant, to account for the system gain. This scaled curve is then multiplied by the range factor R/R_0 to account for the difference in the area of the radar range cell. The scaled and normalized sea clutter attenuation is compared with the measured clutter attenuation in a range interval where the sea clutter is dominant.

The results of these comparisons show that, in the range interval where the ground-wave sea clutter is dominant, the measured and modelled clutter attenuations agree very well over a variety of sea states, thus giving strong supports to the modelled propagation attenuation.

The validation is then conducted by using the signal of a dedicated ship target. This target was tracked along a radial direction of the HFSWR at Cape Race during a period when the sea state was relatively steady. It is found that the validation using the median sea echo is much more effective than that using the dedicated target signal. It is also shown that the median sea echo is more stable than the target signal for the validation.

With the ground-wave propagation attenuation validated, it is also found that the modelled sea clutter attenuation is highly sensitive to the presence of either ionospheric clutter or skywave interference during periods of steady sea states. It is therefore proposed that the sea cluter attenuation be used together with the measured external noise level to establish a baseline for the ground-wave radar signal attenuation.

Significance: Distortions of the ground-wave radar signal by the skywave signal components such as ionospheric clutter and external interference are fairly common in HFSWR. The distortions would cause the measured clutter attenuation to deviate from the modelled sea clutter attenuation. With the modelled ground-wave propagation attenuation validated, the ground-wave radar signal attenuation baseline can be used to detect and subsequently quantify the performance degradations due to the signal distortions.

Future plans: It is recommended that the ground-wave radar signal attenuation baseline be used to detect and quantify any performance degradations due to the presence of ionospheric clutter and/or external interference in any HFSWR systems.

It is also recommended that the proposed ground-wave radar signal attenuation baseline be used to further study, and possibly uncover more of, the distortion behaviours of various forms of ionospheric clutter, including those of the mixed-path.

For operational HFSWR systems, the ground-wave radar signal attenuation baseline can be used to generate a simple yet reliable clutter map that meets the operation needs by indicating the expected range performance of the radar. This baseline can also be used to facilitate the optimized implementations of some signal processing modules in the radar receiver such as the external interference canceller and the radar detector software.

Sommaire

On the feasibility of using measured sea clutter continuum in HFSWR to validate modelled ground-wave propagation attenuation in rough sea

Hank Leong; DRDC Ottawa TR 2012-015; R & D pour la défense Canada – Ottawa; septembre 2012.

Introduction : La modélisation de l'affaiblissement de propagation des ondes de sol HF en mer agitée utilise la théorie de Barrick et le programme GRWAVE. Un essai de validation de la théorie de Barrick et de GRWAVE est mentionné par Larson et Pielou de GEC Marconi, la même entreprise qui a développé GRWAVE. En mesurant directement les pertes sur un trajet maritime dégagé de 164 km au large de la côte sud-ouest de l'Angleterre pendant 14 mois, Larson et Pielou ont montré que la propagation modélisée et les pertes observées sur le trajet concordent bien sur la gamme de fréquences de 5,6 à 22,8 MHz dans divers états de mer. Dans le présent document, nous étudions la possibilité d'utiliser le continuum de clutter de mer entre les lignes de Bragg d'un système radar haute fréquence à ondes de surface (HFSWR) monostatique pour valider l'affaiblissement de propagation des ondes de sol modélisé dans les parties inférieures de la bande HF (3-5 MHz).

L'écho de mer des ondes de sol domine le bruit de fond jusqu'à une distance de 200 km. Cet écho peut toutefois être corrompu par du clutter ionosphérique et du brouillage externe. Par conséquent, on doit chercher des jeux de données HFSWR mesurées qui ne sont pas contaminés par des composantes de signal d'onde ionosphérique. La puissance reçue de l'écho de mer varie en fonction de l'état de mer et de l'affaiblissement de propagation des ondes de sol. Pour un état de mer donné, on constate cependant que la médiane de la moyenne du clutter de mer entre les lignes de Bragg est assez constante à une distance donnée et plutôt monotone sur cette distance. De plus, pour un état de mer donné, on suppose que le coefficient de diffusion de la mer est statistiquement constant. Si on suppose aussi que, pour une mer entièrement levée, l'état de mer est constant sur diverses distances dans une direction donnée, on peut alors utiliser l'affaiblissement mesuré de l'écho de mer des ondes de sol pour valider statistiquement l'affaiblissement de propagation modélisé.

Résultats : On a choisi des jeux de données HFSWR de nuit mesurés aux fréquences radar de 3,1 et 4,1 MHz dans divers états de mer pour tester la faisabilité de la validation proposée. Dans chaque état de mer, on prend en fonction de la distance la médiane des puissances de clutter entre les lignes de Bragg le long d'un faisceau fixe sur certains temps de tenu consécutifs. De plus, pour tenir compte du gain du système, l'affaiblissement de propagation modélisé pour l'état de mer sélectionné est ramené à la puissance du clutter mesuré à une distance choisie (R_0) où l'écho de mer est dominant. La courbe proportionnelle est ensuite multipliée par le facteur de distance R/R_0 pour tenir compte de la différence dans la zone de la cellule de distance du radar. L'affaiblissement du clutter de mer mis à l'échelle et normalisé est comparé à l'affaiblissement du clutter mesuré dans un intervalle de distances où le clutter de mer est dominant.

Les résultats de ces comparaisons montrent que, dans l'intervalle de distances où le clutter de mer des ondes de sol est dominant, les affaiblissements du clutter mesuré et modélisé concordent très bien pour divers états de mer, et confirment ainsi fortement la validité de l'affaiblissement de propagation modélisé.

La validation est ensuite réalisée au moyen du signal d'un navire-cible dédié. Cette cible a été poursuivie le long d'une direction radiale du HFSWR à Cape Race pendant une période où l'état de mer était relativement stable. On a découvert que la validation au moyen de l'écho de mer médian est beaucoup plus efficace que la validation au moyen d'un signal cible dédié. On a aussi montré que, pour la validation, l'écho de mer médian est plus stable que le signal de la cible.

Une fois l'affaiblissement de propagation des ondes de sol validé, on a en outre découvert que l'affaiblissement du clutter de mer modélisé est très sensible à la présence soit de clutter ionosphérique, soit de bouillage par onde ionosphérique pendant des périodes d'états de mer stables. On propose donc l'utilisation conjointe de l'affaiblissement du clutter de mer et du niveau de bruit externe mesuré pour établir un modèle de référence pour l'affaiblissement des signaux radar des ondes de sol.

Portée : Des distorsions du signal radar des ondes de sol par les composants du signal d'onde ionosphérique, comme un clutter ionosphérique et un brouillage externe, sont très fréquentes dans le HFSWR. Les distorsions pourraient causer la déviation de l'affaiblissement du clutter mesuré par rapport à l'affaiblissement du clutter de mer modélisé. Après la validation de l'affaiblissement de propagation des ondes de sol modélisé, le modèle de référence de l'affaiblissement des signaux radar des ondes de sol peut servir à détecter, puis à quantifier, la dégradation des performances en raison des distorsions des signaux.

Recherches futures : On recommande l'utilisation du modèle de référence de l'affaiblissement des signaux radar des ondes de sol pour détecter et calculer toutes dégradations des performances causées par la présence de clutter ionosphérique et/ou de brouillage externe dans des systèmes HFSWR.

On recommande aussi l'utilisation du modèle de référence de l'affaiblissement des signaux radar des ondes de sol proposé pour continuer l'étude, et en apprendre possiblement plus sur les comportements de distorsion de diverses formes du clutter ionosphérique, y compris celles du trajet mixte.

Pour les systèmes HFSWR opérationnels, on peut utiliser le modèle de référence de l'affaiblissement des signaux radar des ondes de sol pour générer une carte du clutter simple et fiable qui répond aux besoins opérationnels en indiquant les performances de distance prévues du radar. On peut aussi utiliser ce modèle de référence pour faciliter les mises en application optimisées de certains modules de traitement des signaux dans le récepteur radar, comme l'éliminateur de brouillage externe et le logiciel du détecteur de radar.

Table of contents

List of figures

List of tables

Ackowledgements

The author would like to thank Dr. Hing C. Chan of Radar Systems Section for his thorough review/editing of the manuscript of this report. His constructive criticism, comments and questions have led to two significant revisions of the original manuscript. The author would also like to thank Dr. Ryan Riddolls also of Radar Systems Section for his review/editing of the final draft of the report, and particularly for his suggestion of using the mean-square wave height equation in [1, p.529] to estimate the wind speed corresponding to the measured wave height. His quick but thorough review and editing are appreciated.

1. Introduction

Most HF Surface Wave Radar (HFSWR) simulation programs model the rough, but electrically conductive, sea surface with the effective surface impedance derived by Barrick [1], and then use it as an input in standard programs such as Grwave [2] to calculate the Basic Transmission Loss (BTL). At DRDC Ottawa, we have been using this approach to model the BTL, but we refer it to as the ground-wave propagation attenuation for reasons explained in Appendix A. The theoretical simulation of HFSWR range performance includes not only the model of ground-wave propagation attenuation, but also models of sea clutter spectra, external noise and radar cross sections (RCS) of targets of interest. For coastal surveillance applications, the radar generally operates in the lower portions of the HF band between 3 and 5 MHz. In this frequency band, the RCS values for two classes of ship targets of interest have been modelled and the aspect-averaged RCS values have been estimated in [3]. Furthermore, the estimated RCS values have been verified in [3] and [4], respectively. Although the sea clutter model has not been validated, the average of the sea clutter continuum between the Bragg lines in which the ships are mostly detected has been empirically related to sea state [5], and the measured performance of the radar in sea clutter has also been studied in [6]. The site-specific CCIR[1] quiet noise model has also been validated with local measurements in [7]. However, there has been no concerted effort to validate the modelled ground-wave propagation attenuation.

In the open literature, there had also been no attempt to satisfactorily validate the ground-wave propagation attenuation in rough sea conditions until Larson and Pielou [8] reported their experiment in 1989. By directly measuring the propagation losses over a 164-km clear sea path off the southwest coast of England over a period of fourteen months, Larson and Pielou concluded that the modelled ground-wave propagation attenuations based on Barrick's theory and Grwave agreed well with the observed path losses over a variety of sea states in the frequency range between 5.6 and 22.8 MHz. No other validation attempt was reported since then, although Pielou and Larson further discussed in 1990 the suitability of various standard sea wave spectral models for path loss prediction on the basis of their previous experimental results [9]. This technical report investigates whether it is feasible to use the sea echo of a monostatic HFSWR system to validate the modelled ground-wave propagation attenuation.

For a HFSWR system looking over an area of the ocean surface, the ground-wave sea echo is a permanent part of the Doppler spectrum. The spectral content of the sea echo comprises of the first- and second-order resonant components and a sea clutter continuum. Figure 1 shows an example of the sea clutter spectrum. The resonant components usually fluctuate significantly with time (radar dwells), but those coming from a fully developed sea (a steady sea state with long duration and fetch) are expected to be statistically constant [10]. However, because of the significant fluctuation, long-time averaging is required to estimate the resonant components. In reality, however, the sea state may not stay the same for long enough for the resonant components to be estimated. Hence, these resonant components are not used in the current validation. Instead, the investigation is focused on using the median of the averaged sea clutter continuum level between the Bragg lines. Here the average of the sea clutter continuum between the Bragg lines is used as an approximation for the average of the entire sea clutter continuum. Physically,

[1] CCIR is the French acronym for International Radio Consultative Committee, the former body of the International Telecommunication Union (ITU).

the sea clutter continuum is considered as the superimposed replicas of the ocean wave spectrum [11], thus representing a superposition of the energies scattered back by the forward and backward ocean waves (except the resonant waves). From the perspective of radar signal processing, the mean level of the sea clutter continuum between the Bragg lines is of key interest, because the ship targets are mostly detected in that Doppler interval. This approximation is justified because the average of the sea clutter spectrum in the Doppler interval between the Bragg lines is generally an order of magnitude larger than the average of the sea clutter continuum at frequencies outside this interval.

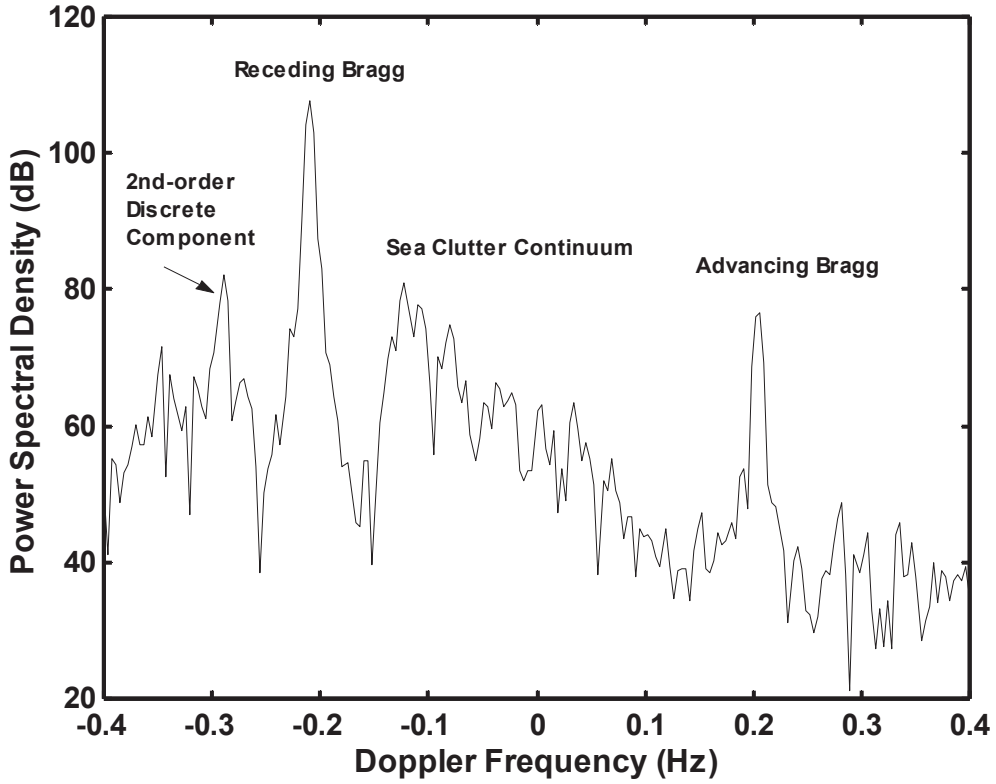

Figure 1 Sea clutter spectrum of HFSWR at the Radar Frequency of 4.1 MHz.

The feasibility study is carried out by using the data measured during TechEval [12] from the DRDC HFSWR at Cape Race, Newfoundland, and the data measured concurrently from the wave buoys operated by the Department of Fisheries and Oceans Canada at the Tail of the Bank and Nickerson Bank. The sea state at a given range in the radar coverage could be indicated by the significant wave height measured by either one of the two wave buoys. The steadiness of the sea state may be indicated roughly by the variations of the measured significant wave heights, or more precisely by the variation of the averaged sea clutter level from the same range itself. An analysis of the data from these indicators later in this report seems to show that the significant wave height measured at the Tail of the Bank was a better indicator than that measured at Nickerson Bank. Hence, we use the significant wave height measured at the Tail of the Bank as a rough indicator for the sea state at a close range where the sea clutter continuum dominates (e.g., 100 km), and then use the variations of the averaged sea clutter between the Bragg lines from this

range bin itself to determine the steadiness of that sea state. If the sea state at the close range is deemed to be steady, then we choose that set of radar data to test the feasibility of the validation.

The measured sea clutter level is estimated from the median of the averaged power levels between the Bragg lines over a selected number of radar dwells in a moving window. The modelled sea clutter attenuation is obtained by calibrating the modelled ground-wave propagation attenuation to the median sea clutter at a selected range bin in the near side of the chosen range interval. The feasibility of the validation will then depend on the closeness between the measured and modelled sea clutter attenuations over the range interval where the sea clutter continuum is dominant.

During TechEval, the Canadian Coast Guard Ship (CCGS) Teleost was used as a dedicated target for the radar at Cape Race, Newfoundland. This report will also validate the ground-wave propagation attenuation using the signal returns from the dedicated target, and compare the effectiveness of the validation with that of using the sea clutter continuum.

The modelled ground-wave propagation attenuation, once validated, can be used with confidence to model the sea clutter attenuation on the assumption that the sea state along the propagation path is constant. The modelled sea clutter attenuation can be used for a couple of important applications. This report will explore, preliminarily, the use of the modelled sea clutter attenuation in these applications.

The remainder of the report is organized as follows. Chapter 2 briefly describes how the sea surface is modelled in the calculation of the ground-wave propagation attenuation. This includes the ocean wave model used, parameter values assumed, and assumptions made in the modelling. Also in Chapter 2, the general characteristics of the modelled propagation attenuation are discussed, and the scope and significance of the validation are specified. After a brief discussion in Chapter 3 on how and when to select the best possible sets of ground-wave radar data from the measured sets of data that are not contaminated with ionospheric clutter and skywave interference, Chapter 4 presents a discussion on sea state, steadiness of sea state, and how to select the best possible sets of ground-wave sea clutter to validate the ground-wave propagation attenuation. Chapter 5 carries out the validation, for a variety of sea states, at both the radar frequencies of 3.1 and 4.1 MHz. Chapter 6 explores the potential applications of the modelled sea clutter attenuation after the validation of the modelled ground-wave propagation attenuation. Finally, Chapter 7 presents the conclusions and recommendations.

2. Characteristics of HF ground-wave propagation attenuation, scope of validation

The effective surface impedance derived by Barrick consists of two terms: the impedance of the sea when the sea surface is perfectly smooth and a second term that accounts for surface roughness [1]. The additional loss due to the second term is simply called the added loss. Barrick [1] shows that the added loss is generally greater for rougher seas, higher frequencies, and longer ranges. Above 5 MHz and at ranges greater than 200 km, the added losses are large and easily measurable. However, below 5 MHz and within the range of 200 km, the added losses in most sea states are fairly small (<4 dB, two-way), and in the lower portions of the HF band[2] (e.g., 2-4 MHz), there is even a small enhancement due to a "trapping effect" [1].

An ocean wave height spectrum is required in the evaluation of the effective surface impedance. This chapter describes briefly the ocean wave height model used, parameter values assumed and assumptions made in the modelling of the ground-wave propagation attenuation. The general characteristics of the modelled ground-wave propagation attenuation and the differences of the added losses are also described, and the scope of the validation is then specified.

2.1 Modelling parameters

Like Barrick in [1], we use the Phillips model [14] for the ocean wave height spectrum. The Phillips model is a semi-isotropic wind-wave spectrum – the model assumes that waves are generated only in the direction to which the wind is going and the wave spectrum is identically zero in the direction from which the wind is coming. The Phillips model also relates the wave height spectrum (W) of a saturated sea at the wind speed, U, to the magnitude of the wave number, κ, as

$$W(\kappa) = \frac{4B}{\pi\kappa^4}, \tag{1}$$

for $\kappa \geq g/U^2$, and $W(\kappa) = 0$ for $\kappa < g/U^2$, where B is the scaling coefficient ($B = 0.005$) and g is the gravitational acceleration ($g = 9.81$ m/s^2). The Phillips model is a simplistic model. For a given wind speed U, The Phillips model assumes an abrupt cut-off in the excitation of ocean waves with wave number κ. For $\kappa < g/U^2$, the model assumes that the waves are not excited, but for $\kappa \geq g/U^2$, the model assumes that the waves are not only excited but also saturated. Note that Phillips model also implies that, to have the ocean waves with a wavelength L saturated, the wind speed must be greater than the square root of $gL/2\pi$. Further discussion of saturated sea will be given in Section 4.1.

Both Barrick's theory and Grwave assume that the propagation medium (i.e., the sea surface) is homogeneous. In the case of propagation over a rough sea, Barrick also assumes that the sea state is uniform across range.

[2] Strictly speaking, HF band is between 3 and 30 MHz and the frequency range of 2-3 MHz is part of the MF band. However, the band of 2-30 MHz here is simply referred to as the HF band.

The conductivity of the smooth sea in North Atlantic is assumed to be 4 S/m, and the dielectric constant is 80.

2.2 Characteristics of ground-wave propagation attenuation

It is well known that the HF ground-wave propagation attenuation has the following characteristics:

1. The ground-wave propagation attenuation at a given sea state increases rapidly with range and radar frequency.

2. The ground-wave propagation attenuation generally increases with sea state, except in the lower portions of the HF band where there could be small enhancements [1].

3. The increases of the ground-wave propagation attenuation with sea state become even larger at higher frequencies and longer ranges.

It is primarily the rapid rise of the ground-wave propagation attenuation with frequency that dictates the operation of HFSWR in the role of coastal surveillance for ship and aircraft targets in the lower portions of the HF band. For example, the HFSWR systems at Cape Bonavista and Cape Race, Newfoundland operated in a dual-frequency mode at 3.1 and 4.1 MHz to detect and track the relatively large cargo container vessels and small 1000-ton ships.

Figures 2 and 3 show the modelled two-way ground-wave propagation attenuation curves, respectively at the radar frequencies of 3.1 and 4.1 MHz, for the sea states with the wind speeds of 0 (smooth sea), 10, 20, 30 and 50 knots. Wind speeds up to 30 knots are fairly common in the North Atlantic, but a wind speed of 50 knots is rare. From Figures 2 and 3, one can observe that the modelled ground-wave propagation attenuations at the two radar frequencies do not change much with sea state within the range of 200 km; only at the extreme wind speed of 50 knots do the differences between the modelled ground-wave propagation attenuations become apparent. Note that the small enhancements due to a “trapping effect” [1] are observable from the modelled ground-wave propagation attenuations for the wind speeds of 10 and 20 knots.

2.3 Characteristics of added losses

The possibility for the radar to resolve the ground-wave propagation attenuations from two different sea states depends on the separation between the added losses. In the HF band between 3 and 5 MHz, the difference between the added losses is not only small, but also varies non-monotonically with sea state. Figures 4 and 5 show the two-way added losses as functions of range for the four non-zero wind speeds, respectively at the two radar frequencies. The magnitudes of the added losses and the small enhancements due to the “trapping effect” are easily observable in Figures 4 and 5. More importantly, the differences among the two-way losses for the sea states at the three lower wind speeds of 10, 20 and 30 knots can also be observed. Within the range of 200 km, these differences are no more than 2 dB at the radar frequency of 3.1 MHz, and no more than 3 dB at the radar frequency of 4.1 MHz. Hence, it is expected to be difficult to resolve these differences by measurements, particularly at the lower radar frequency.

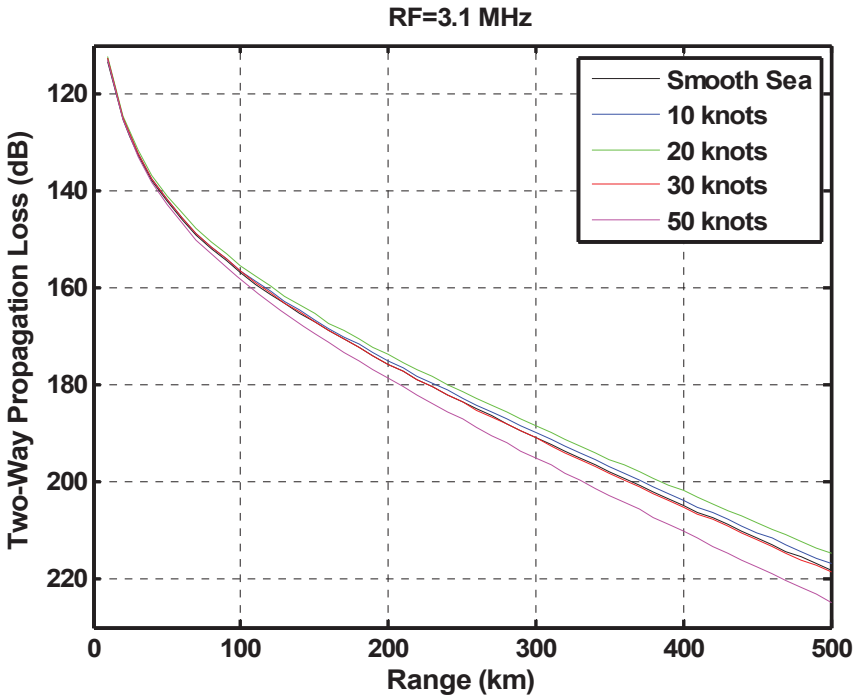

Figure 2 *Modelled two-way propagation losses at the radar frequency of 3.1 MHz for wind speeds of 0, 10, 20, 30 and 50 knots.*

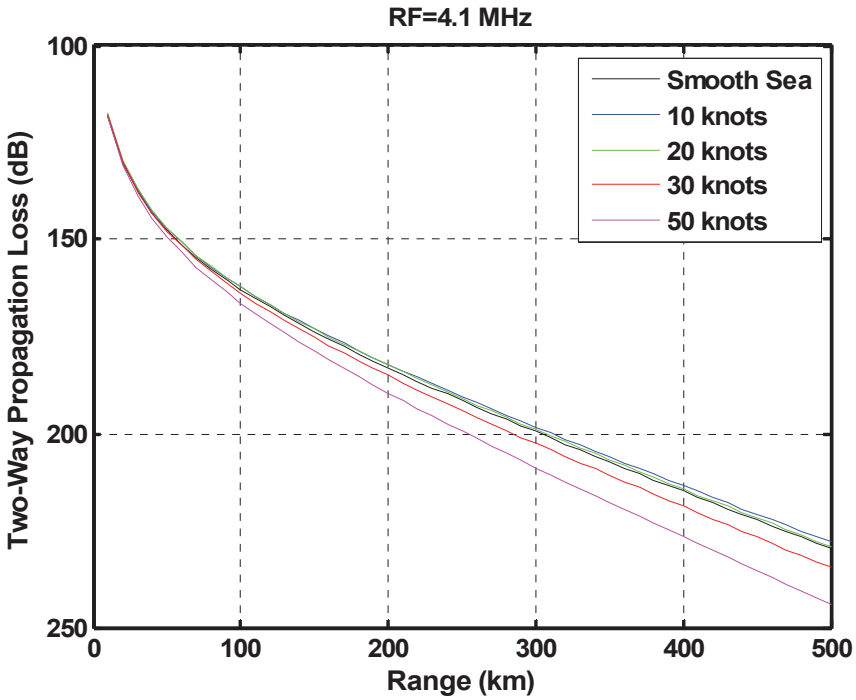

Figure 3 *Modelled two-way propagation losses at the radar frequency of 4.1 MHz for wind speeds of 0, 10, 20, 30 and 50 knots.*

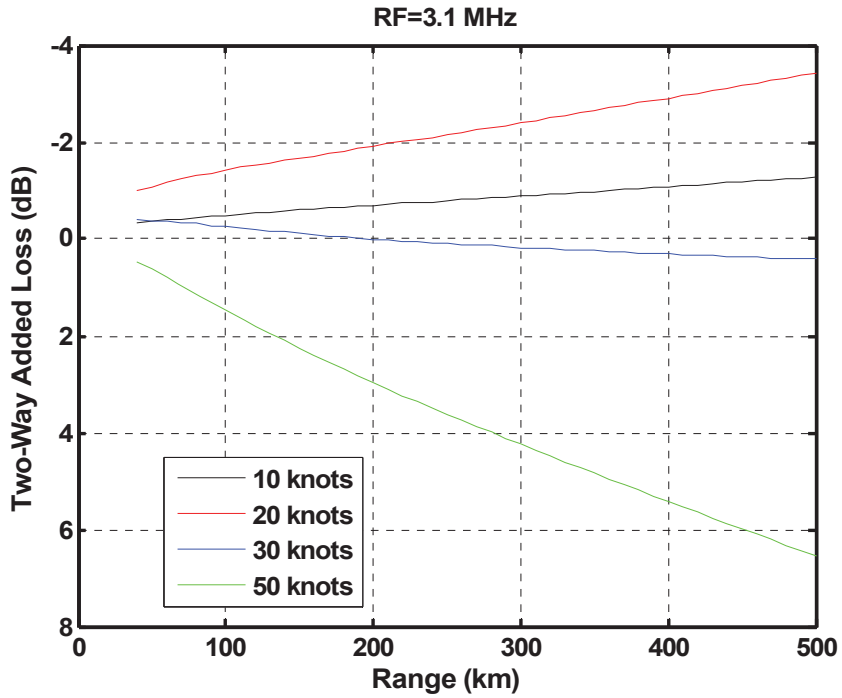

Figure 4 *Modelled two-way added losses at the radar frequency of 3.1 MHz for wind speeds of 10, 20, 30 and 50 knots.*

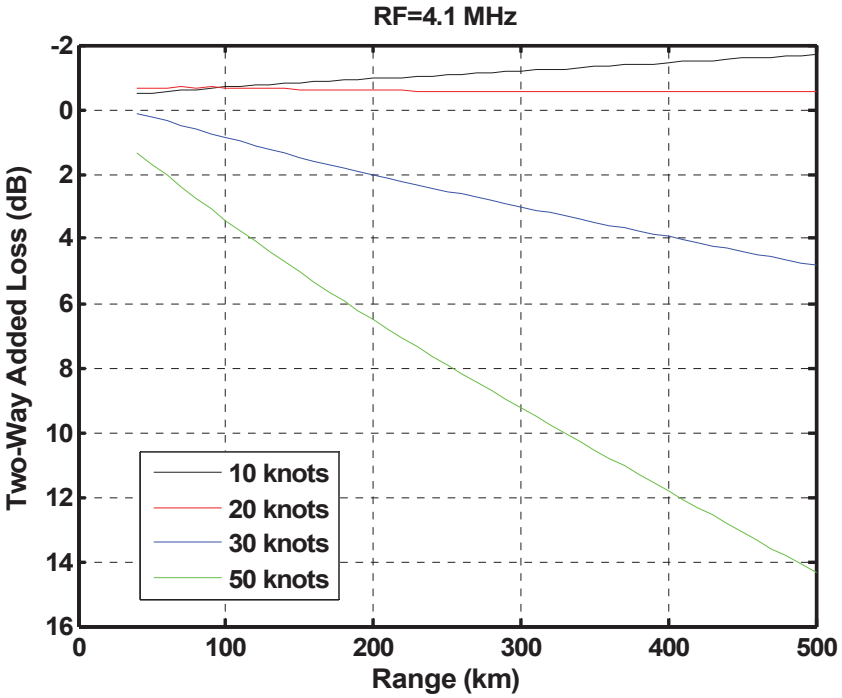

Figure 5 *Modelled two-way added losses at the radar frequency of 4.1 MHz for wind speeds of 10, 20, 30 and 50 knots.*

2.4 Scope and significance of the validation

It should be noted that the purpose of the proposed validation is not to verify the absolute value of the modelled ground-wave propagation attenuation as the overall gain of the radar system was not calibrated, nor to resolve all the differences between the ground-wave propagation attenuations at different sea states as some of these differences are too small to be distinguished by measurements. Rather, it is to verify the general trends of the modelled ground-wave propagation attenuation curves. These trends of the ground-wave propagation attenuation curves, once validated, will greatly facilitate the assessment of the HFSWR performance. Most of the HFSWR simulators do not include models of ionospheric clutter and external interference. Hence, they cannot account for the presence of these extraneous components in the simulation. This report will show that, with the modelled ground-wave propagation attenuation validated, the modelled sea clutter attenuation is very sensitive to the presence of either skywave interference or ionospheric clutter. With a reasonable assumption that the sea state along the propagation path is constant, the modelled sea clutter attenuation can potentially be used to detect the distortions by these skywave signal components, and subsequently quantify the performance degradations due to these distortions.

Here it should be pointed out that most the dominant features of the skywave signal components can be observed with human eyes from the Doppler spectrum. However, it would be difficult for the radar to recognize all the features in the two dimensional space of range and Doppler frequency without human intervention. The modelled sea clutter attenuation has the potential after the validation to be used by the radar to establish a ground-wave radar signal attenuation baseline to detect the presence of either skywave interference or ionospheric clutter autonomously.

3. Selection of non-interfered ground-wave radar data

This chapter briefly discusses how to select the best possible set of ground-wave radar data that is not contaminated with ionospheric clutter and skywave interference to test the feasibility of the proposed validation.

The HFSWR signal comprises of sea clutter, ionospheric clutter, external interference and noise. The sea clutter is propagated via ground-wave, but ionospheric clutter and external interference are propagated via skywave (except local interference). There is also a mixed path clutter where the transmitted radar signal is obliquely bounced off the ionosphere and returned to the radar receiver via surface wave or the transmitted signal is reflected by the ocean waves, bounced off the ionosphere and then returned to the radar receiver. The mixed path clutter is considered as one form of the ionospheric clutter.

In the absence of ionospheric clutter and external interference, the ground-wave propagated sea clutter could dominate over background noise at ranges up to 200 km. However, during daytime, the clutter reflected off the E layer in the ionosphere is present in a narrow range interval centered at about 110 km when the radar frequency is below the critical frequency to the E layer. Hence, preferably, the nighttime radar data are used to test the feasibility of the validation. However, at night, there could be external skywave interference. Hence, to validate the trend of the modelled ground-wave propagation attenuation uninterruptedly in the interval between the minimum instrumentation range of the radar (62.5 km) and ~200 km, we need to find the data from those measured at night that were not distorted by external interference.

One efficient way to find the data that were not distorted by external interference is by plotting the intensity of the averaged power level between the Bragg lines along a fixed beam as a function of range and time (dwell number). Figure 6 shows such intensity plots of the data measured by the radar at Cape Race at the radar frequencies of 3.1 and 4.1 MHz along the boresight direction of the receive array over the range of coverage and over nearly a full day of data measurement. The time axis in Figure 6 is referenced to 00:00 on February 9, 2002 in Coordinated Universal Time (UTC), which is 3.5 hours ahead of the local non-daylight-saving time[3]. The radar started to record data at approximately 22:00 on Feb 8, 2002. From the 3.1-MHz radar channel, severe interference could be observed until about 08:00, and then there was no interference for over 4 hours before the sunrise at about 12:00. Hence, the non-interfered ground-wave sea echo measured between 08:00 and 12:00 from the 3.1-MHz channel can potentially be used in the validation. The 4.1-MHz radar channel was relatively clear and as shown in Figure 6(b), the ground-wave sea echo was the only dominant component at ranges up to 200 km, throughout the nighttime period. Hence, all the nighttime 4.1-MHz radar data can potentially be used to test the feasibility of the proposed validation. Note that the dominant component at the far ranges was the ionospheric clutter from the F layer. In general, the critical height of the F layer increases gradually as the night progresses, reaches the maximum within 1-2 hours after the local midnight, and then decreases gradually as the day approaches. Figure 6(b) shows that, in the period between 04:00 and 08:00, the ground-wave sea echo could dominate over a longer range interval because of the higher critical height of the F layer. Hence, to test the

[3] Unless specified otherwise, the time in UTC will be used hereafter in this report.

feasibility of the validation, the preference is to use the data segment in the period between 04:00 and 08:00.

All the non-interfered nighttime radar data are collected together and sorted according to the sea state. The final selection of the data from the collection to test the feasibility of the validation is subject to the steady sea state requirements discussed in the next chapter.

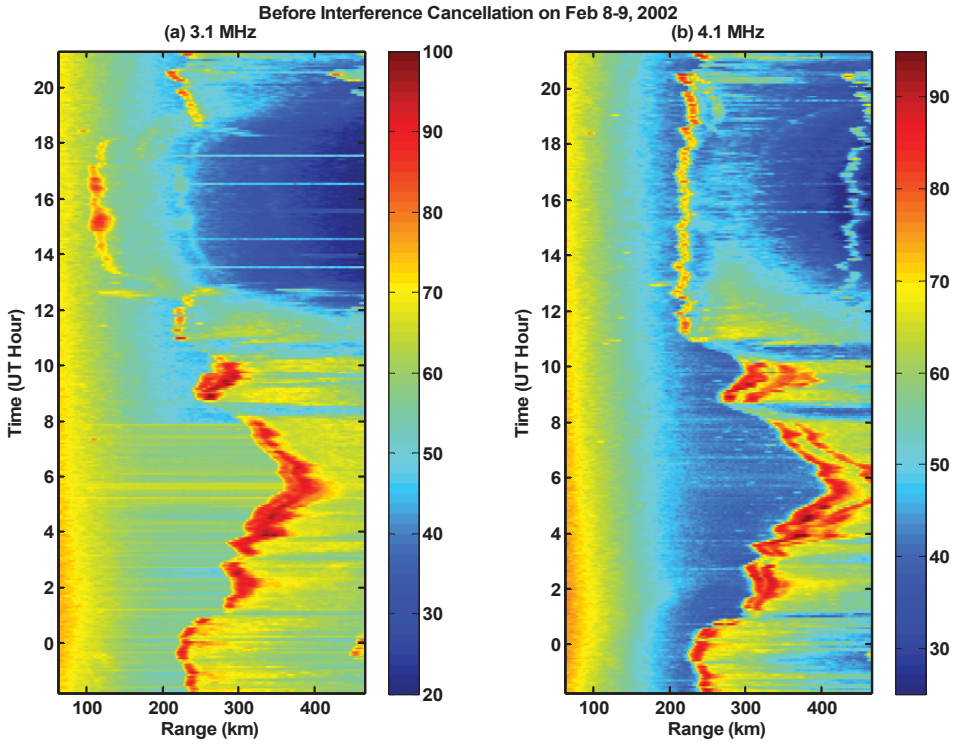

Figure 6 *Averaged background signal intensities between Bragg lines along a fixed beam at the radar frequencies of 3.1 and 4.1 MHz.*

4. Selection of ground-wave sea clutter and validation approach

This chapter presents a discussion on sea state, steadiness of sea state, and how to select the best possible sets of ground-wave sea clutter to test the feasibility of the validation. The validation approach and a set of validation procedures are also described.

4.1 Ocean wave saturation

In general, the ocean waves would grow with the wind, with energy being transferred from the wind to the waves [14]. However, the growth of the wind and waves cannot continue indefinitely. At a given wind speed, the transferred energy to the waves could be lost due to wave breaking and other dissipation. If the energy being added to the waves is equal to the energy being dissipated, then the ocean waves are saturated and the sea is fully developed.

The ocean wave saturation is considered as a steady sea state, and it is achieved when the wind blows at a constant velocity long enough and over sufficient fetch. Here, the fetch refers to the horizontal distance over an open ocean over which a nearly constant wind has been blowing. The estimated wind durations, fetches and wind speeds required to fully develop seas are provided in the International Mariners' Codes in Table 12.1 of [10]. The IMC suggest that, to generate a fully developed sea at a level between Rough and Very High, the wind duration required is in the order of 20-30 hours and the fetch required is in the order of 150-500 nautical miles (275-900 km). This implies that, under the fully developed sea conditions, the sea state is essentially constant for a very long duration and uniform across range over a very long distance. The homogeneous medium requirement that is assumed in the modelling of the ground-wave propagation attenuation is therefore satisfied under the fully developed sea conditions. It would be ideal then to use the radar echoes from a fully developed sea to validate the modelled ground-wave propagation attenuation.

However, in practice, the fully developed sea conditions are not likely attainable as it is nearly impossible for the wind to blow at a constant velocity for such long time and distance. Hence, a less restrictive but more practical approach is needed to select the sea clutter data to test the feasibility of the validation. This will be discussed in Section 4.5.

There is also a wind speed requirement for the resonant ocean waves to be saturated. The Phillips model states that for a given wind speed U, the saturated waves are limited to those with wave numbers $\kappa \geq g/U^2$. The first-order resonant waves have a wavelength L equal to one half of the radar wavelength λ. Hence, the minimum wind speed required for the first-order resonant waves to be saturated is given by

$$U_{min} = \sqrt{\frac{cg}{4\pi f}}. \qquad (2)$$

where c is the speed of light ($c = 3x10^8$ m/s) and f is the radar frequency. At the radar frequencies of 3.1 and 4.1 MHz, the minimum wind speeds required are 8.7 and 7.6 m/s (17 and 15 knots), respectively.

4.2 Sea state and steadiness of sea state

The sea state in the coverage of the radar at Cape Race could be monitored by the data measured from either one of the two wave buoys operated by the Department of Fisheries and Oceans Canada. The two wave buoys were located respectively at Nickerson Bank (46.4° N, 53.4° W) and Tail of the Bank (43.7° N, 51.7° W). Figure 7 shows the locations of the two wave buoys relative to that of the radar. The two wave buoys provided hourly measurements of the ocean wave spectra and wind velocities at the two locations. Appendix B shows the significant wave heights measured from the two wave buoys for the radar measurement periods during TechEval. A comparison of all the wave heights indicates that the variation patterns were generally similar, but the significant wave height measured from the Tail of the Bank was mostly higher than that from Nickerson Bank, particularly during periods of high sea states. Nickerson Bank was at a distance of about 25 km from the shoreline, and the Tail of the Bank was at a distance of about 346 km from the radar (also from the shoreline). The higher sea state was likely caused by the fact that the wave buoy at the Tail of the Bank was much farther away from the shore.

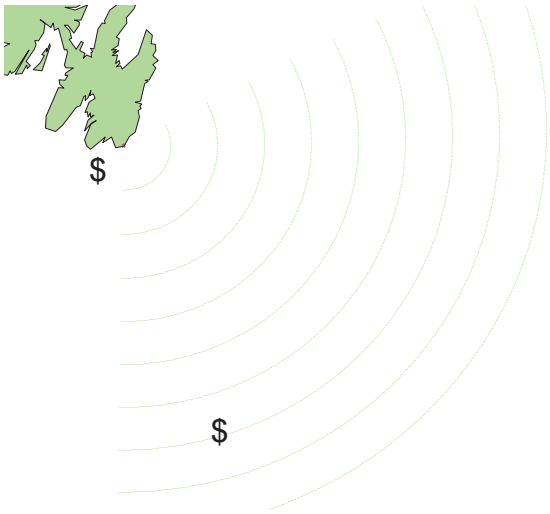

Figure 7 *Relative locations of the wave buoys at the Tail of the Bank (far side) and Nickerson Bank (close range) to the potential coverage area of the HFSWR at Cape Race, Newfoundland.*

The steadiness of the sea state in the radar coverage could also be monitored roughly by the variation of the significant wave height measured by either one of the wave buoys. However, a more precise indicator for the steadiness of the sea state in a selected radar resolution cell is the variation of the measured power level of the sea clutter continuum between the Bragg lines from that radar cell itself. The significant wave height (H_s) is conventionally defined as the average of the heights, measured from crest to trough, of the 1/3 highest waves, and it is measured as four times the standard deviation (σ_z) of the water surface elevation [15]. Our previous investigation [5] related the average power of the sea clutter continuum between the Bragg lines at a close

range (taken from 85% of the central portion of the Doppler spectrum between the Bragg lines) to the value of σ_z measured by an *in situ* wave buoy at the same location. The results of this investigation show that, at 3.1 MHz, the averaged sea clutter power between the Bragg lines is roughly proportional to the fourth power of σ_z. In the absence of an *in situ* wave buoy, however, this empirical relationship cannot be used to determine the value of σ_z in the region of interest from the averaged clutter level. Nevertheless, the variation of this averaged sea clutter level can be used to indicate more precisely the steadiness of the sea state in the selected radar cell.

Both the previous and the current investigations are based on the hypothesis that the scattering coefficient of the sea echo from a given sea state is statistically constant. An example is given below to illustrate the steadiness of the medians of the averaged sea clutter continuum levels between the Bragg lines, and the correlations of these medians with the significant wave heights at the Tail of the Bank and Nickerson Bank. Figure 8 shows the significant wave heights from the two wave buoys measured approximately during the same period as the radar data in Figure 6. Figures 9 and 10 show the averaged sea clutter levels between the Bragg lines measured over the same period from the radar resolution cell at the range of 90 km along the boresight direction at the radar frequencies of 3.1 and 4.1 MHz, respectively. The medians of these averages were taken over a moving window of 21 dwells (~1.5 hours), and these are also shown in Figures 9 and 10 (in red). From Figures 9 and 10, one can observe that, while the average sea clutter powers fluctuated from dwell to dwell, the medians of the averages were actually fairly steady.

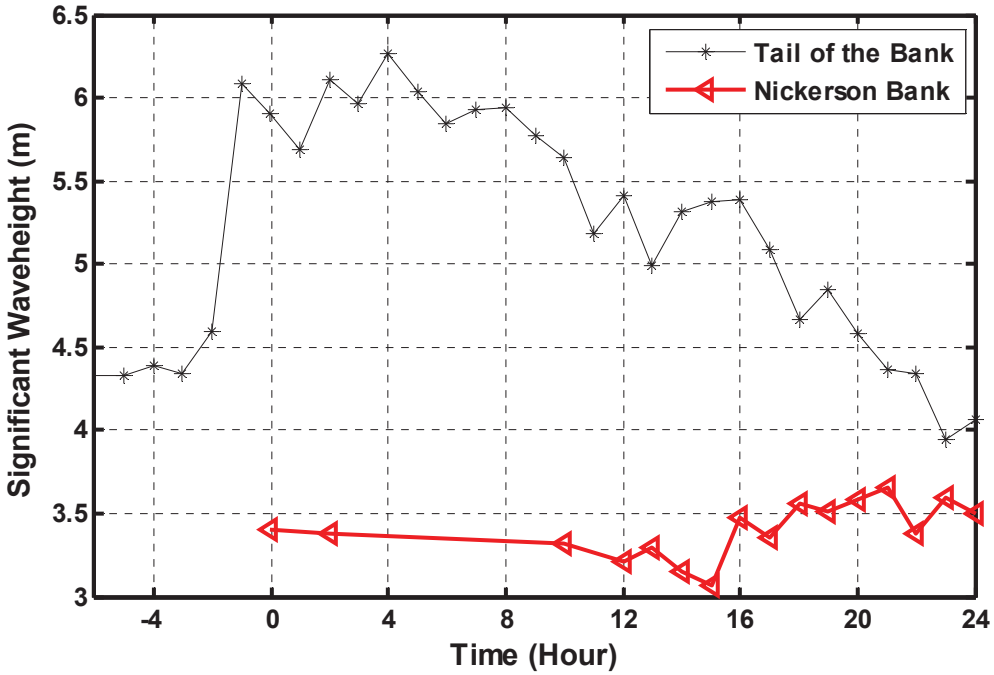

Figure 8 *The significant wave heights recorded on February 9, 2002.*

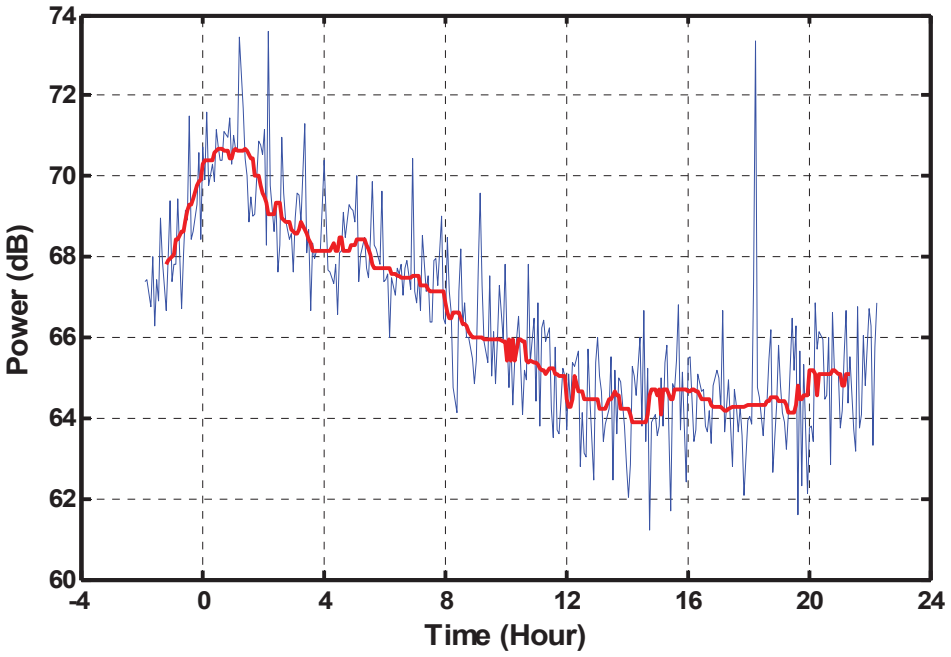

Figure 9 *The averaged sea clutter between Bragg lines measured on February 9, 2002 at the frequency of 3.1 MHz at the range of 90 km along the boresight direction.*

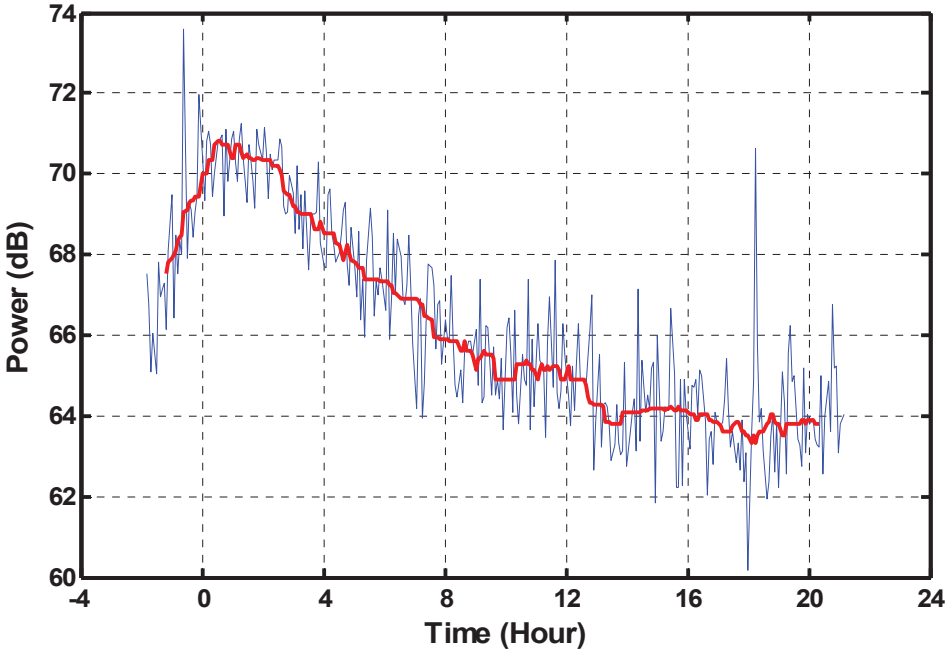

Figure 10 *The averaged sea clutter between Bragg lines measured on February 9, 2002 at the frequency of 4.1 MHz at the range of 90 km along the boresight direction.*

It should be noted here that the reason for which the median, instead of the mean, of the averaged sea clutter is used is to avoid possible bias by the strong returns caused by the interference from a local ionosonde (e.g., at ~18:00 in the dataset shown in Figures 9 and 10).

Figures 9 and 10 show that there were actually several time intervals in which the medians of the averaged sea clutter were nearly constant. For example, the median deviated within ±0.5 dB of its mean in the time intervals approximately between 00:00 and 02:00, 03:45 and 06:00, 08:00 and 11:00, and 12:00 and 19:30 at the radar frequency of 3.1 MHz, and between 00:00 and 03:00, 09:00 and 12:15, and 13:00 and 20:15 at the radar frequency of 4.1 MHz. All these time intervals are longer than the duration over which the median is estimated. It is believed that the sea states during these time intervals were more likely uniform across range than during others. Hence, in this report, the radar data from these time intervals are selected to investigate the feasibility of the proposed validation.

From Figure 8, one can observe that the sea state indicated by the significant wave height from the Tail of the Bank rose rapidly between -02:00 and -01:00 (i.e., 1-2 hours before 00:00) and stayed relatively steady for about 8 hours before falling off slowly. The medians of the averaged sea clutter levels also exhibited this pattern of rise and fall for the sea state level in the radar cell at the range of 90 km. However, the fine details of the variation patterns indicated by the sea clutter levels did not always match those indicated by the significant wave height measured from the Tail of the Bank. For example, the duration of the risen sea state as indicated by the significant wave height measured from the Tail of the Bank at about 00:00 was much longer than those observed from the two sea clutter levels. Another example is that the variation patterns of the sea state between 12:00 and 20:00 as indicated by the two sea clutter levels appeared to match that observed from Nickerson Bank better than the Tail of the Bank.

The observations in the two examples above suggest that the sea state in the radar cell at the range of 90 km was initially influenced by the sudden rise of the ocean wave field at the Tail of the Bank and that the sea state level rose up and then gradually settled towards the sea state level at Nickerson Bank, the latter of which was fairly constant.

Despite the differences, the data in Figures 8-10 show that the significant wave height at the Tail of the Bank was a better indicator for the sea state in the radar cell than that at Nickerson Bank. Hence, in this report, we use the significant wave height measured at the Tail of the Bank as a rough indicator for the overall sea state in the radar coverage.

4.3 Measured sea clutter attenuation

The variations of the average clutter level along a fixed beam are examined with respect to range. For a given sea state over a single radar dwell, this average may fluctuate wildly with range, and the range attenuation of this average may not be monotonic even in the sea-clutter-dominated range interval. However, over a number of consecutive dwells, it is observed that the median of these averages quickly becomes stable, and the range attenuation of the median in the sea-clutter-dominated range interval generally becomes monotonic. Figure 11 illustrates this by plotting the medians of the average clutter, taken from the same beginning of a data segment but over four different durations of one, 11, 21 and 31 dwells, as functions of range at the radar frequency of 3.1 MHz. As shown in Figure 11, the average clutter fluctuates fairly wildly with range, but the

median becomes stable fairly quickly. When the duration is increased to 31 dwells, the attenuation of the median has become fairly monotonic, at ranges up to 180 km. It is decided then that for the 3.1-MHz channel, the median of the averaged sea clutter levels between the Bragg lines is taken over every 31 dwells (2.26 hours).

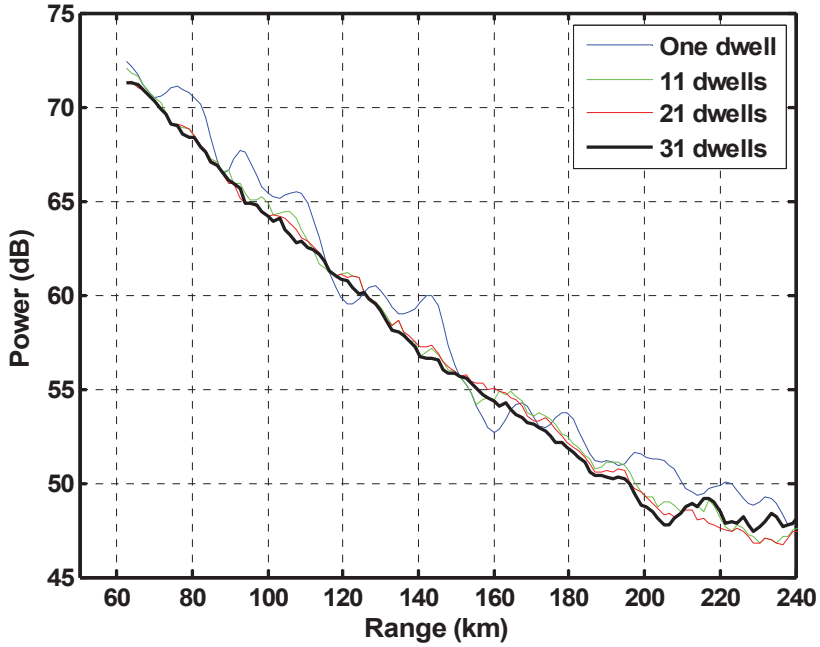

Figure 11 *Range attenuations of the medians of the average sea clutter between Bragg lines taken over one, 11, 21 and 31 radar dwells at 3.1 MHz.*

Note that the sea clutter in this data segment appears to dominate at ranges approximately up to 160 km only because of a low level of external interference. Beyond 160 km, the external interference and noise gradually become more dominant as the sea clutter continues to decrease.

Similarly, Figure 12 plots the medians of the average clutter taken from the same beginning of a data segment measured at the radar frequency of 4.1 MHz over three durations of one, 11 and 21 dwells. An even faster convergence to stability can be observed in Figure 12 for the 4.1-MHz data. The attenuation of the median in this latter case becomes fairly monotonic when the duration is increased to 21 dwells (1.52 hours).

Note also that the sea clutter in this latter segment appears to dominate at ranges up to 200 km, but beyond 200 km, the external noise and external interference gradually become more dominant as the sea clutter continues to decrease.

The attenuation of the median above in the ranges where the sea clutter is dominant is simply referred to as the measured sea clutter attenuation. In the next section, the modelled ground-wave propagation attenuation and the measured sea clutter at a selected range where the second-order sea clutter continuum is known to be dominant are used to derive the sea clutter attenuation. This is referred to as the modelled sea clutter attenuation.

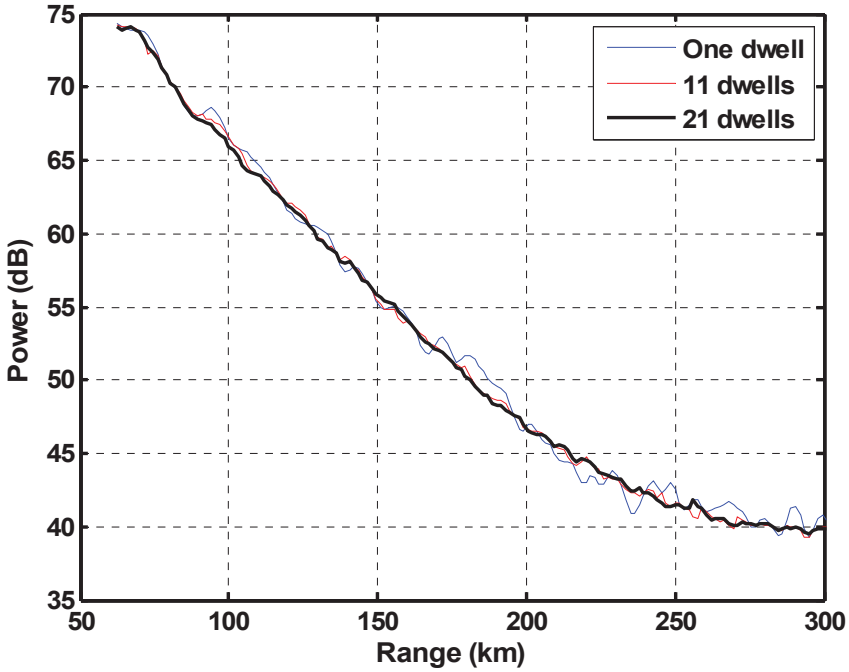

Figure 12 *Range attenuations of the medians of the average sea clutter between Bragg lines taken over one, 11 and 21 radar dwells at 4.1 MHz.*

4.4 Modelled sea clutter attenuation

The ground-wave sea clutter power received from the monostatic HFSWR can be calculated using the ground-wave radar range equation:

$$P_s(R) = \Gamma\left(\frac{4\pi}{\lambda^2}\right)\left(\frac{\sigma_s}{L_b^2}\right), \tag{3}$$

where Γ is the product[4] of the transmit power (P_t), and transmit and receive antenna gains (G_t and G_r) divided by the miscellaneous system loss (L_m), and L_b is Grwave's one-way basic transmission loss.

If the miscellaneous system loss (L_m) is constant across range, then the only parameters that are range dependent on the right-hand side of Equation (3) are σ_s and L_b. At a selected range R_o where the sea clutter is known to be dominant, the sea clutter power P_s can be approximated with the measured spectral power between Bragg lines at the beamformed output of the radar receivers, P_r. Hence, Equation (3) can be written as

[4] It should be noted here that the absolute gain of the radar system is irrelevant for the proposed validation. The readers are referred to [13] for a discussion of different forms of radar range equation, antenna gain and radar cross section.

$$P_r(R_o) \approx P_s(R_o) = \Gamma\left(\frac{4\pi}{\lambda^2}\right)\left(\frac{\sigma_s(R_o)}{L_b^2(R_o)}\right). \quad (4)$$

Assuming that the sea state is uniform across the propagation path, the RCS of the sea echo from a monostatic HFSWR is given by

$$\sigma_s = \sigma_o A, \quad (5)$$

where A is the area of the ocean patch in the radar cell given by

$$A = R\,\Delta\theta\,\Delta R, \quad (6)$$

where R is the target range, ΔR is the range resolution of the radar and $\Delta\theta$ is the azimuthal beamwidth of the receive antenna array.

Dividing Equation (3) by Equation (4), and using the relationships in Equations (5) and (6), we obtain

$$P_s(R) = P_r(R_o)\left(\frac{L_b(R_o)}{L_b(R)}\right)^2\left(\frac{R}{R_o}\right). \quad (7)$$

Hence, by using the received power at the selected range R_0 as a calibration point, the sea clutter attenuation can be calculated from the modelled ground-wave propagation attenuation. (The readers are referred to Appendix A for more discussion about the relation between Grwave's and Barrick's BTL.)

4.5 Feasibility study

The objective of the current report is to investigate the feasibility of using the measured sea clutter continuum in HFSWR to validate the modelled HF ground-wave propagation attenuation. The measured sea clutter attenuation is thus compared with the modelled sea clutter attenuation across the range interval where the sea clutter is known to be dominant to test the feasibility of the validation, on the basis of the assumption that the sea state is constant across the range interval. The assumption is made in order to meet the requirement that the propagation medium is homogeneous. This requirement can be met if the sea is fully developed. However, the fully developed sea conditions are not likely attainable in practice. Hence, a less restrictive but more practical approach is used to choose the sea-clutter data from the collection of non-interfered nighttime radar data for the validation investigation. As previously mentioned, the variation of the median sea clutter level at a close range (e.g., 100 km) can be used to indicate the steadiness level of the sea state at that range. Hence, for each sea state, as gauged roughly by the significant wave height at the Tail of the Bank, we choose a set of sea-clutter data that have steady median sea clutter levels at the close range, and we test the feasibility of the validation by comparing the measured and modelled sea clutter attenuations over the range interval where the second-order sea clutter is dominant.

Specifically, the following set of procedures is used to select the sea-clutter data from the radar data collection and then to validate the ground-wave propagation attenuation:

1. For each sea state, as determined by the significant wave height measured at the Tail of the Bank, we search through the data log from TechEval for the availability of nighttime non-interfered radar data at that sea state.

2. If there are nighttime non-interfered radar data available at that sea state, we then search through the data for segments that have steady sea-clutter medians at a specified range bin on the near side of the range interval where the sea clutter is dominant. For the median at the close range to be steady, its variation over a selected time interval (typically the duration of the median) is limited to no more than 0.5 dB from its mean.

3. If there is a data segment that meets the requirements above, we then make the assertion that the sea state is uniform across range, and we use the wind speed corresponding to the significant wave height to simulate the ground-wave propagation attenuation. Note that this assertion is made here only because of the homogeneous propagation medium assumed in the modelling of the ground-wave propagation attenuation. It should also be noted that the wind speed corresponding to the significant wave height can be either calculated by solving the mean-square wave height equation in [1, p. 529] or looked up by using the IMC in [10]. With $H_s = 4\sigma_z$, the calculated wind speed is found to be ~10% higher than the looked-up value. It is noted that Ref. 10 was published a year after Ref. 1, but to be consistent with Barrick's formulation in [1], we choose the calculated wind speed to simulate the ground-wave propagation attenuation in this report.

4. The median of the sea clutter power for the data segment is then taken for all the range bins in the radar coverage. The portion of the median curve in the range interval where where the sea clutter continuum between the Bragg lines was dominant (approximately between 63 and 200 km) represents the measured sea clutter attenuation. The duration over which the median is taken is heuristically determined, as discussed in Section 4.3.

5. The modelled sea clutter attenuation is calculated as per Section 4.4.

6. The measured and modelled sea clutter attenuations are then compared to investigate the feasibility of the proposed validation.

7. If the root-mean-square value of the difference between the attenuation curves (to be defined in next chapter) is within a certain limit (e.g., 0.5 dB), then we conclude that the validation is feasible and that the ground-wave propagation attenuation is statistically validated.

In essence, we choose the best possible sets of sea-clutter data to meet the requirement made in the modelling assumption. If there is a close agreement between the measured and modelled sea clutter attenuations in range, then we draw the conclusions as indicated in Step 7 above.

5. Validation of ground-wave propagation attenuation

Four sets of the HFSWR data, measured at each of the radar frequencies of 3.1 and 4.1 MHz, were selected for four different sea states according to the selection guidelines given in the two chapters above, i.e., the data were selected from those measured at night when the F-layer clutter appeared as far as possible, when there was no external interference, and when the sea state was steady as per Section 4.5. Tables 1 and 2 list the selected sets of data for this validation purpose at the two radar frequencies in the four different sea states.

Table 1 Selected HFSWR data at 3.1 MHz

Date of Measurement	**Dwell No.**	**Measurement Period (UTC in hh:mm)**	H_s **(m)**	**Wind Speed (knots)**	**Sea State**
April 2, 2002	175-205	08:49 – 11:04	2.6 – 2.7	22	Rough
Feb 14, 2002	1-31	22:43 – 00:58	2.7 – 2.9	23	Very Rough
Feb 9, 2002	280-310	18:41 – 20:56	4.3 – 4.7	29	High
Feb 9, 2002	154-184	09:18 – 11:33	5.2 – 5.6	32	High+

Table 2 Selected HFSWR data at 4.1 MHz

Date of Measurement	**Dwell No.**	**Measurement Period (UTC in hh:mm)**	H_s **(m)**	**Wind Speed (knots)**	**Sea State**
May 30, 2002	20-30	20:18 – 23:22	0.6 - 0.7	11	Slight
Jan 5, 2002	80-100	20:03 – 21:35	2.8 - 3.0	23	Very Rough
Jan 5, 2002	30-50	04:31 – 06:03	4.1 – 4.3	28	High
Feb 9, 2002	100-120	05:25 – 06:57	5.8 – 5.9	33	High+

The durations of the datasets were chosen as short as possible so that the sea state in the range interval of interest could be approximately maintained throughout. Each of the datasets at the radar frequency of 3.1 MHz was measured consecutively over a period of 31 dwells (2.26 hours), and each of the datasets at the radar frequency of 4.1 MHz was measured over a period of 21 dwells (1.52 hours). As discussed in Section 4.3, these durations were deemed to be sufficient for the medians of the average sea clutter to be stable.

All the datasets were taken from periods when the sea states, as indicated by the medians of the averaged sea clutter at the range of about 100 km, were relatively steady. The sea states were roughly indicated by the corresponding bands of significant wave heights (H_s) measured from the wave buoy at the Tail of the Bank. The lower and upper bounds of this small band are the minimum and maximum of the significant wave heights measured in the period between the hour immediately before the beginning of each dataset and the hour immediately after the end of the dataset (The wave buoy output data once every hour.). As shown in Tables 1 and 2, the difference between the lower and upper bounds is no more than 0.4 m among all the datasets.

The mid-value of each significant-wave-height band was then mapped into a sea state description in accordance with the IMC given in Table 12.1 of [10]. The sea states for the selected datasets range from Slightly Rough to High+. The High+ sea state is given to those with significant wave

heights just slightly below the boundary between High and Very High Sea States, which is 20 feet (6.1 m) according to the IMC.

The mid-value of each significant-wave-height band is also used in the mean square wave height equation [1, p. 529] to calculate the corresponding wind speed:

$$\sigma_z^2 = \frac{BU^4}{2g^2}, \tag{8}$$

where g is the gravitational acceleration, B is a scaling constant ($B \approx 0.005$) and U is the wind speed. The mean square wave height is equal to the total area underneath the ocean wave height spectrum and above zero height. The equation above is derived by using the Phillips wave height spectrum for a fully developed sea. With $H_s = 4\sigma_z$, the corresponding wind speeds for the 3.1-MHz datasets are calculated to be 22, 23, 29 and 32 knots, and the corresponding wind speeds for the 4.1-MHz datasets are calculated to be 11, 23, 28 and 33 knots. These corresponding wind speeds are then used in the simulation of the respective ground-wave propagation attenuations for the four sea states at the two radar frequencies.

As discussed in Chapter 3, it is desirable to choose the radar data measured during periods near midnight when the altitude of the F layer was the highest. Hence, an attempt was made to search for the data measured near midnight. However, it was discovered that skywave interference was almost always present at night in the 3.1-MHz radar channel. The only exceptions were in the period of 2-3 hours either before dawn or after dusk. It is often observed that there is little or no skywave interference for the period of 2-3 hours before dawn (e.g., in the data shown in Figure 6), and occasionally observed that there is little or no skywave interference for the period of 2-3 hours after dusk. Subsequently, the selected data for the 3.1 MHz channel were all measured in these two time periods.

The two sets of 4.1-MHz radar data chosen for the higher sea states were measured during periods near midnight. However, in the lower sea states, low level ionospheric clutter was unexpectedly found during nighttime at ranges corresponding to, or slightly greater than, the normal height band of the E layer. This low level ionospheric clutter altered the statistics of the sea clutter in the 4.1-MHz radar channel, particularly in the range interval between 100 and 120 km. An attempt was then made to find two alternate sets of data measured at night at different times. These are shown in Table 2 for the two lower sea states.

All but one set of the radar data were taken before any External Interference Cancellation (EIC). The radar used a phase-coded pulse waveform to generate a matched and a mismatched channel from the output of each receive antenna. The matched channel is expected to receive the radar echo and external interference, but the mismatched channel is expected to receive the interfering signals only. The EIC algorithm used the outputs from the matched and mismatched channels to estimate the interference component in the matched channel, and a subtraction of the estimated interference component from the output of the matched channel would then lead to a cancellation of the interference. It was of a concern that the EIC might change the statistics of the sea clutter due to a small leakage of the radar clutter into the mismatched channel. Hence, EIC was performed only when necessary. This was the case for the Very Rough sea state at the radar frequency of 3.1 MHz.

We are now ready to validate the modelled ground-wave propagation attenuation. The measured sea clutter was taken from the median of the average sea clutter between Bragg lines (in linear scale, within 85% of the Bragg frequencies) over the duration of the selected dataset. The wind speed corresponding to the mid-value of the small significant-wave-height band was used in the modelling of the ground-wave propagation attenuation. The modelled propagation attenuation was then scaled to the median of the average sea clutter at a range (R_0) where the sea clutter was dominant, and the scaled propagation attenuation was normalized by the range factor R/R_0 to account for the increase, as a function of range, in the radar resolution cell size. Finally, the scaled and normalized propagation attenuation was compared with the measured sea clutter attenuation to test the feasibility of the validation.

It should be noted that the range R_0 can be arbitrarily chosen from the range interval where the sea clutter is dominant. Initially, this range was chosen to be 100 km for all the datasets. However, it was later discovered that in some of the nighttime datasets selected above, there was still the presence of a very low level of E-layer clutter at that range. In these exceptional cases, a closer range was then picked for the calibration of the propagation attenuation.

To gauge the closeness between the measured and modelled sea clutter attenuations, the root-mean-square (rms) value of the difference between the two curves (both in decibel scale) is defined as

$$\Delta_{rms} = \sqrt{\frac{\sum_{n=n_1}^{n=n_2} \left(P_r(R_n) - P_s(R_n)\right)^2}{n_2 - n_1 + 1}}, \tag{8}$$

where n is the range bin index with $n_1 = 13$ and $n_2 = 66$, corresponding in range to approximately between 80 and 160 km. Note that the values of n_1 and n_2 here have been chosen after the comparisons of the measured and modelled sea clutter attenuation over many sets of HFSWR data. It is observed that the measured sea clutter was often slightly lower than the modelled sea clutter in the first few range samples in the radar coverage, due to incomplete pulse compression at ranges less than 74 km. Therefore, the first 12 range samples are excluded from the rms calculation. Note that the range of 74 km corresponds to the 8th range sample; four more range samples are excluded to give a round-off range of 80 km on the near side of the range interval. The data beyond the range bin of 66 are also excluded because the sea clutter beyond the range of 160 km is no longer dominant, particularly in low sea states.

The remaining sections of this chapter are organized as follows. Sections 5.1 and 5.2 present the validation results in the order from high to low sea states for the two radar frequencies of 3.1 and 4.1 MHz, respectively. In Section 5.1, Figures 13-16 show the comparisons for the 3.1-MHz radar in the four sea states. Similarly, in Section 5.2, Figures 17-20 show the comparisons for the 4.1-MHz radar. Unless specified otherwise, the calibration range R_0 is chosen to be 100 km throughout this report. The rms values for all the cases are tabulated, and the validation results are then summarized in Section 5.3. Finally, in Section 5.4, we compare the effectiveness of the proposed validation with that using a dedicated ship target.

5.1 Measured and modelled sea clutter attenuations at 3.1 MHz

5.1.1 Sea state: High+

Significant wave height: 5.2 – 5.6 m

Corresponding wind speed: 32 knots

Observations:

There is an excellent agreement between the measured and modelled sea clutter attenuation at range up to 160 km. The rms value of the difference between the ranges of 80 and 160 km is only 0.269 dB.

Small deviations exist in the ranges of 160-200 km because the sea clutter level is diminishing and the external interference-plus-noise is becoming dominant.

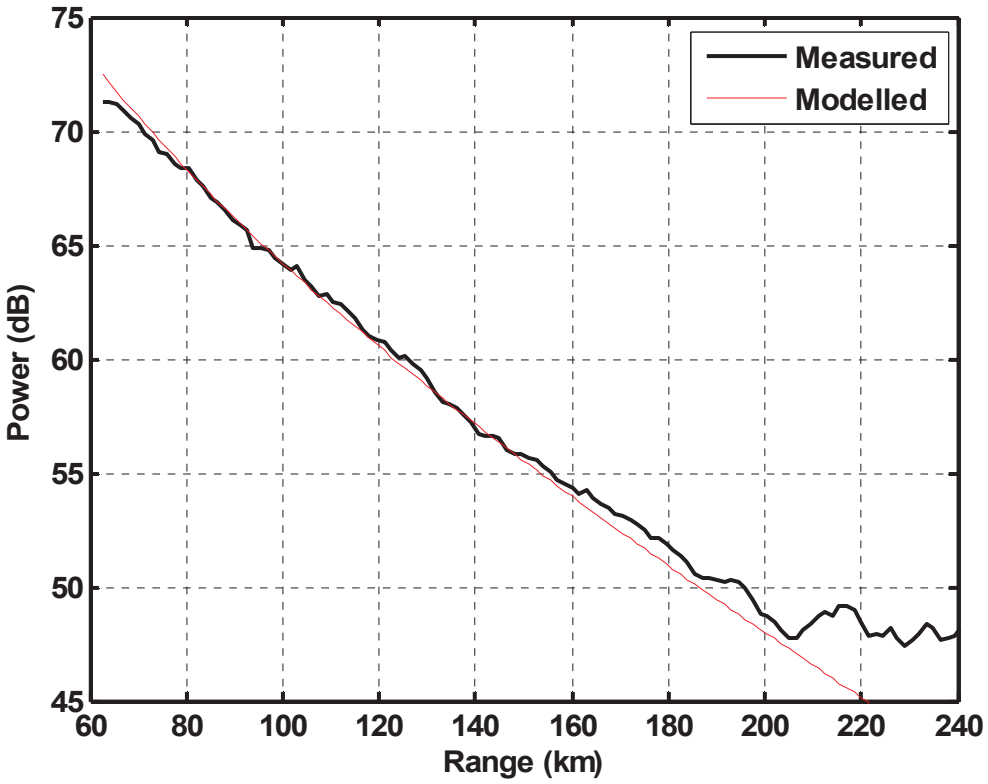

Figure 13 *Comparison between modelled and measured ground-wave sea clutter attenuation at 3.1 MHz (sea state: High+).*

5.1.2 Sea state: High

Significant wave height: 4.3 – 4.7 m

Corresponding wind speed: 29 knots

Observations:

The calibration range R_0 was moved to 90 km after a small bump was observed at the range of 100 km.

There is also an excellent agreement between the measured and modelled sea clutter attenuation at range up to 200 km. The rms value of the difference between the ranges of 80 and 160 km is only 0.318 dB.

The sudden increase in the measured data at ranges beyond 200 km was caused by the ionospheric clutter from F layer.

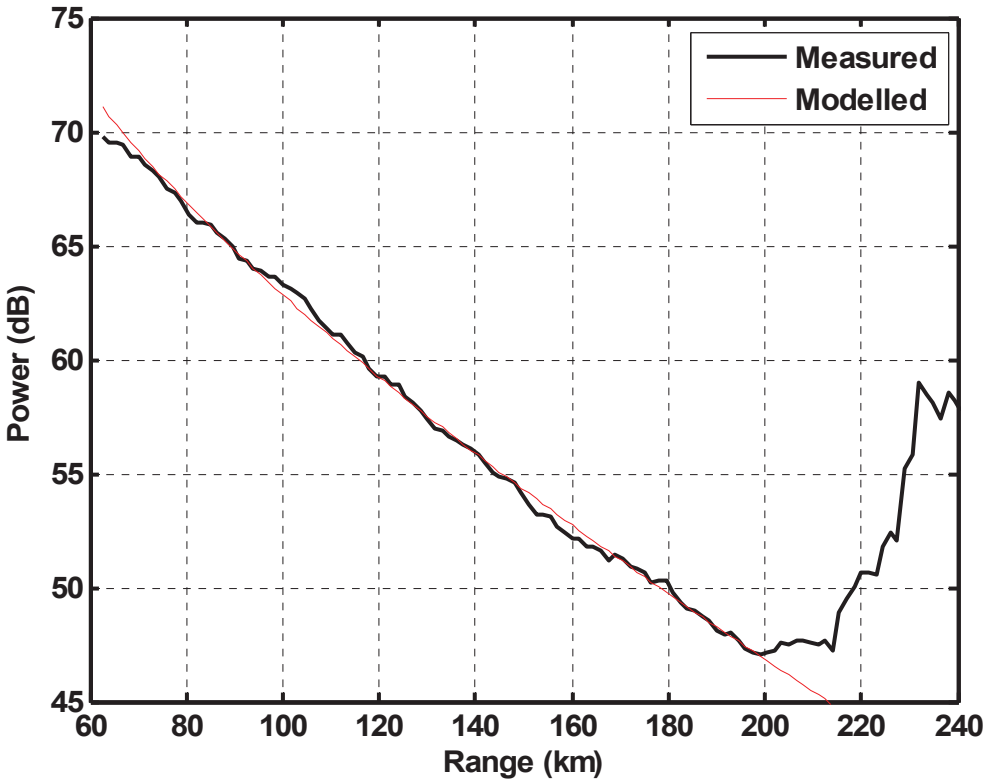

Figure 14 *Comparison between modelled and measured ground-wave sea clutter attenuation at 3.1 MHz (sea state: High).*

5.1.3 Sea state: Very Rough

Significant wave height: 2.7 – 2.9 m

Corresponding wind speed: 23 knots

Observations:

A reasonably close agreement between the measured and modelled sea clutter attenuation is reached, at range up to 170 km. The rms value of the difference between the ranges of 80 and 160 km is 0.303 dB.

The EIC was performed on the measured radar data. The deviations at ranges beyond 170 km were due to by residual interference.

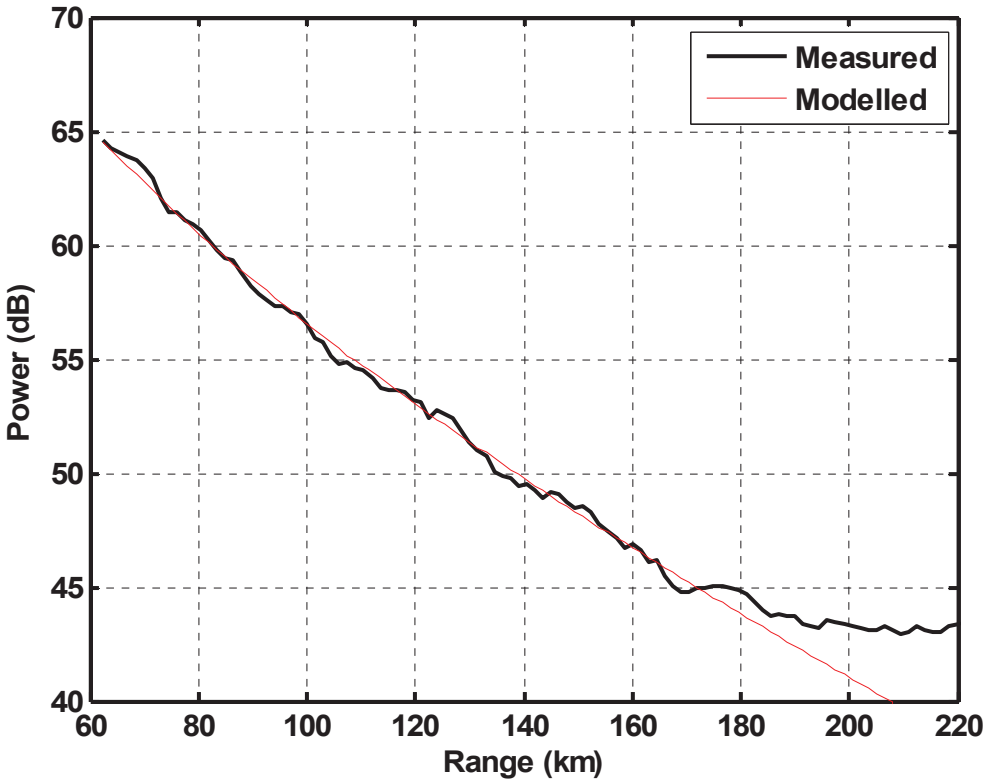

Figure 15 *Comparison between modelled and measured ground-wave sea clutter attenuation at 3.1 MHz (sea state: Very Rough).*

5.1.4 Sea state: Rough

Significant wave height: 2.6 – 2.7 m

Corresponding wind speed: 22 knots

Observations:

A reasonably close agreement between the measured and modelled sea clutter attenuation could be observed at range up to 180 km. The rms value of the difference between the ranges of 80 and 160 km is only 0.326 dB.

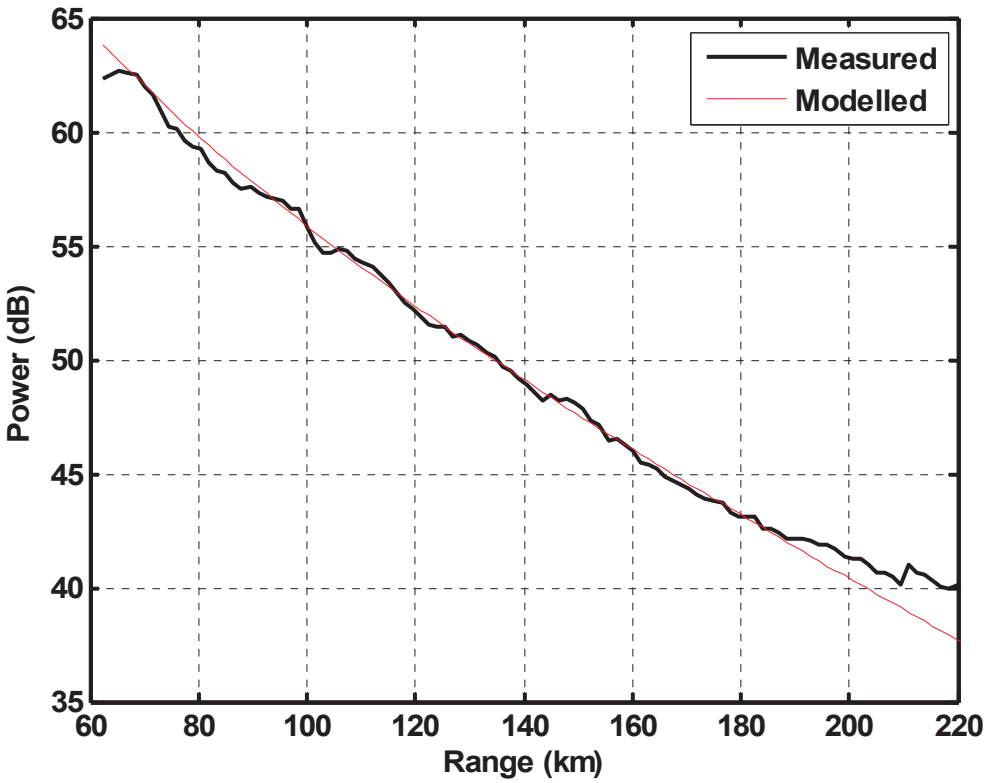

Figure 16 *Comparison between modelled and measured ground-wave sea clutter attenuation at 3.1 MHz (sea state: Rough).*

5.2 Measured and modelled sea clutter attenuations at 4.1 MHz

5.2.1 Sea state: High+

Significant wave height: 5.8 – 5.9 m

Corresponding wind speed: 33 knots

Observations:

There is an excellent agreement between the measured and modelled sea clutter attenuation at ranges up to 192 km. The rms value of the difference between the ranges of 80 and 160 km is only 0.281 dB.

Small deviations exist beyond 192 km because the sea clutter level is diminishing and the external interference-plus-noise is becoming dominant.

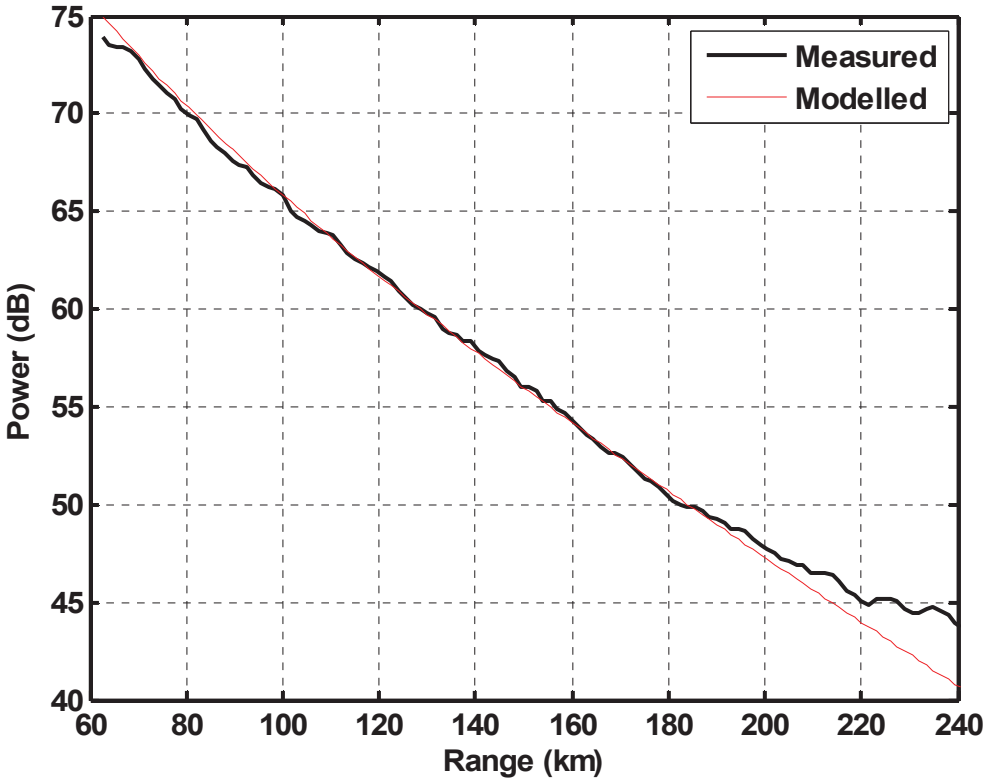

Figure 17 *Comparison between modelled and measured ground-wave sea clutter attenuation at 4.1 MHz (sea state: High+).*

5.2.2 Sea state: High

Significant wave height: 4.1 – 4.3 m

Corresponding wind speed: 28 knots

Observations:

There is a very good agreement between the measured and modelled sea clutter attenuation in the range interval between 100 and 165 km.

However, the measured data might have been slightly biased because of the occasional appearance of the clutter from E layer. As a result, small deviations are observed at ranges less than 100 km.

The deviations at ranges beyond 165 km are again caused by the fact that the sea clutter level is diminishing and the external interference-plus-noise is becoming dominant.

The rms value of the difference between the ranges of 80 and 160 km is 0.415 dB.

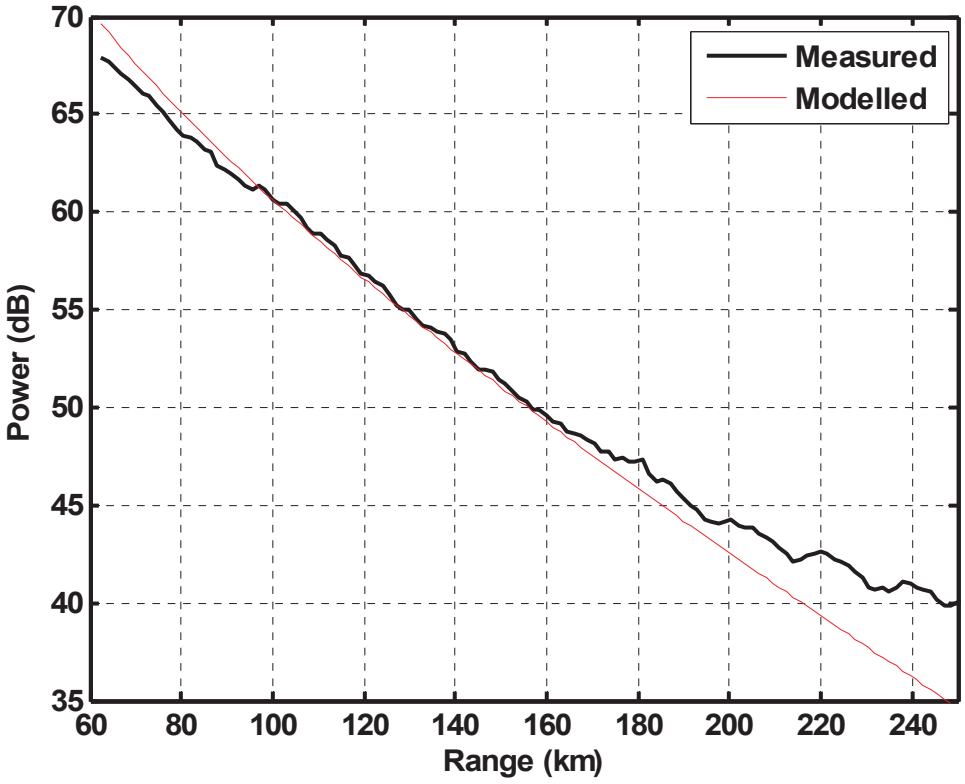

Figure 18 *Comparison between modelled and measured ground-wave sea clutter attenuation at 4.1 MHz (sea state: High).*

5.2.3 Sea state: Very Rough

Significant wave height: 2.8 – 3.0 m

Corresponding wind speed: 23 knots

Observations:

The calibration range R_0 was moved to 90 km after a small bump was observed between the ranges of 100 and 160 km, likely due to the presence of ionospheric clutter from the E layer. This will be discussed further in the next chapter.

The measured and modelled sea clutter attenuation curves agree well at ranges less than 100 km. However, the measured sea clutter attenuation curve is slightly higher in the range interval between 100 and 160 km. Between 160 and 185 km, the two curves agree reasonably well again. The rms value calculated over the entire interval of 80-160 km is 1.225 dB, but if we exclude the data biased by the E-layer clutter from the calculation, i.e., we use the data from the ranges between 80 and 100 km and from the ranges between 160 and 185 km only, the rms value is equal to 0.389 dB.

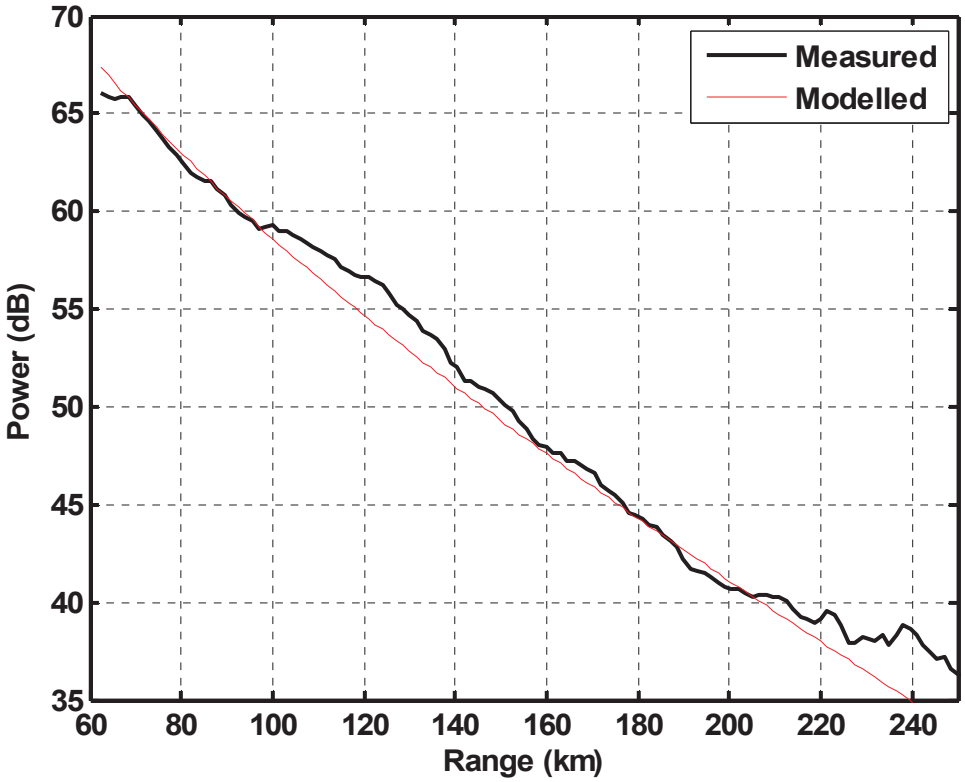

Figure 19 *Comparison between modelled and measured ground-wave sea clutter attenuation at 4.1 MHz (sea state: Very Rough).*

5.2.4 Sea state: Slightly Rough

Significant wave height: 0.6 – 0.7 m

Corresponding wind speed: 11 knots

Observations:

While a reasonably close agreement is achieved in the range interval between 80 and 155 km, there are deviations at ranges less than 80 km and at ranges beyond 155 km. These deviations were likely caused by an uneven sea, i.e., the sea state was not uniform across range.

The rms value, still calculated using the data between the ranges of 80 and 160 km, is 0.479 dB.

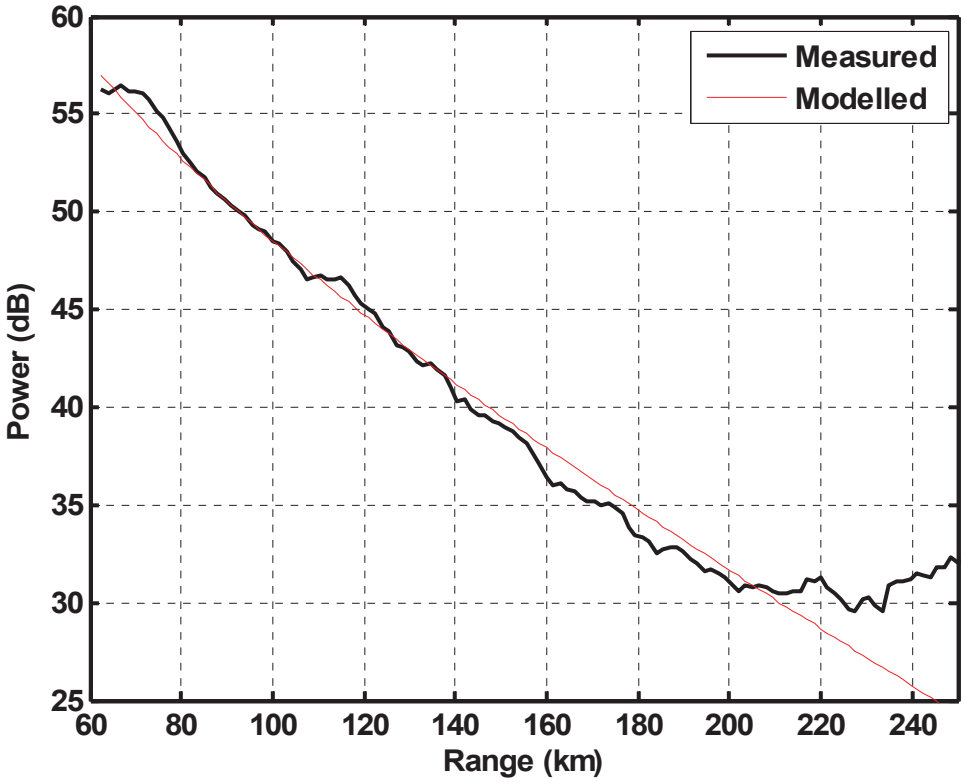

Figure 20 *Comparison between modelled and measured ground-wave sea clutter attenuation at 4.1 MHz (sea state: Slight).*

5.3 Validation Summary

Tables 3 and 4 show the rms values of the differences between the measured and modelled sea clutter attenuations for the cases presented above.

Table 3 RMS difference between measured and modelled sea clutter at 3.1 MHz

Sea State	Corresponding Wind Speed (knots)	Δ_{rms} (dB)
High+	32	0.269
High	29	0.318
Very Rough	23	0.303
Rough	22	0.326

Table 4 RMS difference between measured and modelled sea clutter at 4.1 MHz

Sea State	Corresponding Wind Speed (knots)	Δ_{rms} (dB)
High+	33	0.281
High	28	0.415
Very Rough	23	0.389*
Slightly Rough	11	0.479

The rms values were all calculated using the sea clutter data between the ranges of 80 and 160 km except that in the case of very rough sea at the radar frequency of 4.1 MHz, the rms value of 0.389 dB (marked with * in Table 4) was calculated using the data in the range interval between 80 and 100 km and in the range interval between 160 and 185 km.

The results in the two sections above indicate:

1. There is an excellent agreement between the measured and modelled sea clutter attenuation curves when the sea state is High$^+$ (wind speed > 30 knots). The rms value of the differences between the two curves at either one of the two radar frequencies is less than 0.30 dB.

2. There is a very good agreement between the measured and modelled sea clutter attenuation curves when the sea state is High (30 knots > wind speed > 25 knots). The rms value of the differences between the two curves at the radar frequency of 3.1 MHz is about 0.32 dB. The rms value of the differences between the two curves at the radar frequency of 4.1 MHz is slightly biased by the presence of weak E-layer clutter, and this rms value is about 0.42 dB.

3. There is also a reasonably good agreement between the measured and modelled sea clutter attenuation curves when the sea state is Rough or Very Rough (25 knots > wind speed > 20 knots). The rms value of the differences between the two curves at the radar frequency of 3.1 MHz is about 0.3 dB. The rms value of the differences between the two

curves at either one of the two radar frequencies is less than 0.40 dB, after the E-layer clutter data are excluded from the calculation.

4. The deviation between the measured and modelled sea clutter attenuation curves increases slightly when the sea state level is lower than Rough (wind speed < 20 knots), likely due to an uneven sea. Nevertheless, the rms value of the differences between the two curves at the radar frequency of 4.1 MHz is less than 0.48 dB.

Based on these results, it is concluded that the trend of the modelled propagation attenuation is statistically validated. The above observations show that the higher the sea state, the better the agreement between the measured and the modelled sea clutter attenuations.

The results for the radar frequency of 3.1 MHz appear to be better than those for the radar frequency of 4.1 MHz, because the median at 3.1 MHz was taken over a longer duration than that at 4.1 MHz and because the 4.1-MHz radar data were slightly biased by a low level of ionospheric clutter from the E layer. A shorter duration was used for the median at 4.1 MHz because of the bias.

5.4 Validation using a dedicated target

Alternatively, the validation of the ground-wave propagation attenuation can be carried out using a dedicated ship target. This requires the target to travel at a constant heading and velocity along a radial direction of the radar. The target signal attenuation can be modelled by simply scaling the modelled ground-wave propagation attenuation to the received power of the target at a selected range from the target track, and the modelled target signal attenuation can then be compared with the measured target signals along the target track for the validation. Generally, one ship track is required for each sea state. Hence, this validation approach could become expensive if the validation is to be conducted for all the sea states.

The assumption behind this validation approach is that the RCS of the target is constant. The accuracy of this validation approach therefore depends on the capacity of the ship maintaining constant heading and velocity along a radial direction of the radar. If the heading and velocity are not maintained, the validation would not be accurate because of the aspect variation of the target RCS and because of the Doppler smearing of the target signal.

The set of the data measured during the CCGS Teleost's outbound leg of the TechEval trials [12] can be used to compare the effectiveness of this validation approach with that of the validation using the second-order sea clutter. The outbound portion of the Teleost trial happened to occur during a period when the sea state was relatively steady, with the significant wave height measured at the Tail of the Bank varying in a small range interval between 3.75 and 4.34 m which corresponds to a sea state with a wind speed of ~27 knots. The ground-wave propagation attenuation was then simulated for the sea state with a wind speed of 27 knots. Figure 21 shows the received target signal power along the outbound track and the modelled target signal attenuation, the latter of which was obtained by simply scaling the modelled ground-wave propagation attenuation to the received target signal power at the selected target range of ~170 km. Several disadvantages of this approach using a dedicated target can be observed from Figure 21:

1. The measured target signal power deviates slightly from the modelled target signal attenuation when the target was gradually getting into the heading position at the beginning of the outbound track.

2. The estimated target signal power at the range of ~180 km is inaccurate, likely due to a false alarm.

3. The estimated target signal at the range of ~205 km is lowered due to Doppler smearing. The ship's itinerary data log indicates that the ship slowed down at that time.

4. The estimated target signal power at the far ranges of the track becomes jittery because the signal-to-noise-plus-interference power ratio is low.

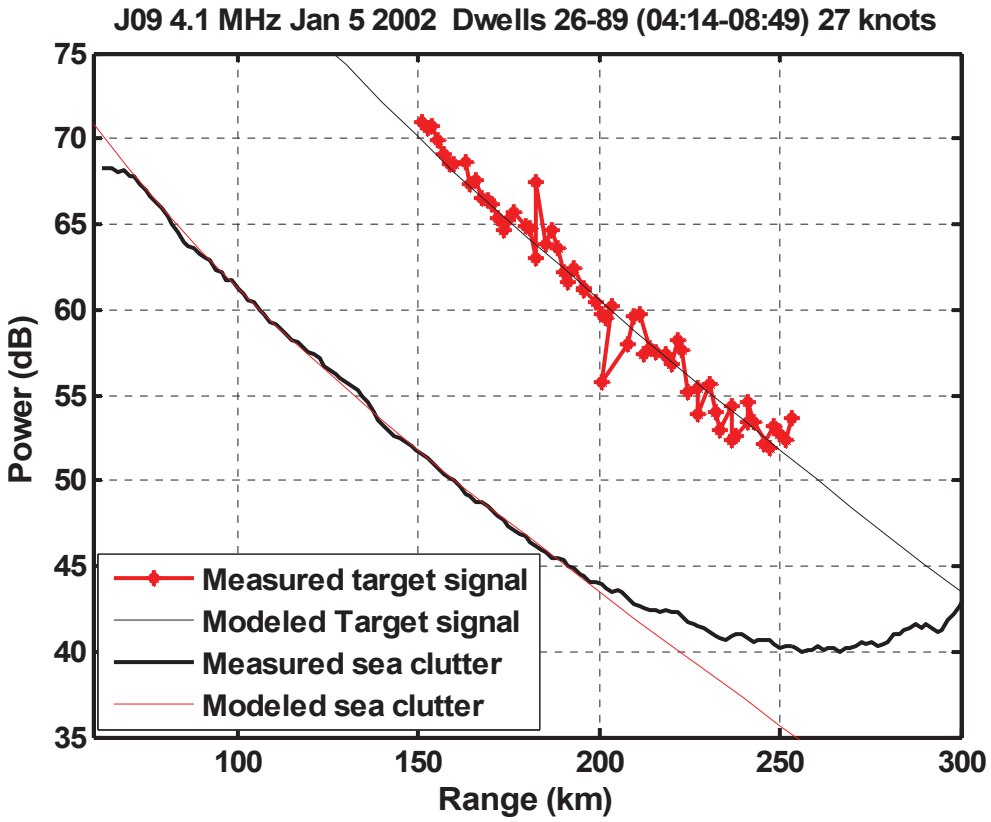

Figure 21 Validations of ground-wave propagation attenuation with target signal and sea clutter

The measured and modelled sea clutter attenuations over this same period are also shown in Figure 21. Note that the measured sea clutter attenuation is smoother than those previously presented because the median of the average clutter levels is taken over a longer period (4.5 vs. 1.5 hours). The results here show that there is a much better agreement between the measured and modelled sea clutter attenuations than that between the measured and modelled target signal

attenuations. The rms difference between the measured and modelled sea clutter attenuations, also calculated between the ranges of 80 and 160 km, is 0.245 dB only. However, the rms difference between the measured and modelled target signal attenuations calculated over the entire target track is 1.14 dB. Note that the range of the calibration for the modelled sea clutter attenuation is set at 100 km.

The results in Figure 21 clearly show that the second-order sea clutter is a much better validating parameter than the dedicated target signal.

6. Potential applications of modelled sea clutter attenuation after validation

Once validated, the modelled ground-wave propagation attenuation can be used to model the sea clutter attenuation. The modelled sea clutter attenuation can then be potentially used for remote sensing of steady high sea states, and more importantly, to facilitate the detection of radar signal distortions caused by ionospheric clutter and/or external interference. These potential applications are preliminarily discussed in this chapter.

6.1 Remote sensing of steady high sea states

For the modelled sea clutter attenuation above, we have relied on the significant wave height measured by the wave buoy at the far range of the radar coverage to select the corresponding wind speed and sea state, and then to predict the added loss for that sea state on the basis of Barrick's formulation. We have also relied on the variation of the median of the average sea clutter levels between the Bragg lines at a close range (e.g., 90 or 100 km) to ensure the sea state was steady. The results above show that the modelled and measured sea clutter attenuations are remarkably close, with an rms difference of no more than 0.5 dB between them. However, it was also pointed out in Section 2.2 that the differences between the added losses modelled for the sea states with the commonly observed wind speeds (10, 20 and 30 knots) within the range of 200 km are also very small. One may ask then: in the absence of the wave height information, can the measured sea clutter attenuation be used to resolve the added losses modelled for the different sea states, i.e., with the assumption that the sea state across the propagation path is constant, can the measured sea clutter attenuation be used to match with one of the modelled sea clutter attenuations for different sea states and therefore determine the sea state in the region of interest?

To answer this question, we need to evaluate the rms values of the differences between the added losses in the same range interval of 80-160 km, and compare these rms values with those of the differences between the modelled and measured sea clutter attenuations calculated in the previous chapter.

Denote the added losses modelled for two selected wind speeds as P_1 and P_2. Similar to the definition in Equation (8), the rms value of the difference between the two modelled curves is defined as

$$\delta_{rms} = \sqrt{\frac{\sum_{n=n_1}^{n=n_2}\left(P_1(R_n) - P_2(R_n)\right)^2}{n_2 - n_1 + 1}}, \tag{9}$$

where the same range bin interval is used, i.e., $n_1 = 13$ and $n_2 = 66$, corresponding in range approximately between 80 and 160 km. Table 5 shows the rms values of the difference between the added losses modelled for any two of the three wind speeds (10, 20 and 30 knots) at the two radar frequencies of 3.1 and 4.1 MHz.

Table 5 shows that, in many cases, the separations between the added losses for any two of the sea states are not much larger than the separations between the measured and modelled sea clutter attenuations for either of the two sea states. In fact, the separation between the added losses for the wind speeds of 10 and 30 knots at the radar frequency of 3.1 MHz, and the separation between the added losses for the wind speeds of 10 and 20 knots at the radar frequency of 4.1 MHz are even smaller than the rms differences between the measured and modelled sea clutter attenuations at either of the corresponding wind speeds. Hence, the added losses in these cases are inseparable.

However, Table 5 also shows that the added loss modelled for the wind speed of 30 knots at the radar frequency of 4.1 MHz is clearly separable from the other two, if we set the minimum separation between the added losses required is equal to the maximum of the rms values between the measured and modelled sea clutter attenuations above (i.e., 0.5 dB). Hence, the radar operating at the frequency of 4.1 MHz can potentially be used as a remote sensor for the steady high sea states (with wind speed $\geq$ 30 knots).

Table 5 RMS difference between two added losses

Wind Speeds (knots)	**δ_{rms} (dB) at 3.1 MHz**	**δ_{rms} (dB) at 4.1 MHz**
10 and 20	0.494	0.0615
20 and 30	0.669	0.894
10 and 30	0.179	0.946

This sea-state sensing process is further illustrated in Figure 22. The sea clutter attenuation curves modelled for the wind speeds of 10, 20 and 30 knots are shown in Figure 22, along with the measured sea clutter attenuation for the High$^+$ sea state when the radar operated at 4.1 MHz. Note that the modelled ground-wave propagation attenuations are all calibrated to the range of 100 km. Figure 22 shows that the sea clutter attenuation modelled for the wind speed of 30 knots clearly matches better with the measured sea clutter than the other two. In the range interval between 140 and 220 km, the curve modelled for the wind speed of 30 knots follows the measured curve closely while the other two modelled curves overestimate the measured sea clutter. Table 6 shows the rms value of the difference between the measured sea clutter and each of the modelled sea clutter curves for the three wind speeds. It is not surprising that the difference between the measured sea clutter and the one modelled for the sea state with the wind speed of 30 knot is the smallest. Hence, by the curve matching, we determine that the sea state was roughly in the High$^+$ range.

The differences between the added losses for the different sea states generally increase as the radar frequency increases. Hence, one can reasonably conclude that it is possible to use this curve matching technique to remotely determine steady high sea states when the radar operates in the absence of ionospheric clutter and external interference at or above the frequency of 4.1 MHz.

It should be noted, however, that in the example above, the curve matching technique is used to determine the level of a high sea state only on the basis of the assumption that the sea state level

is constant in range. If the sea state level is not constant in range, this simple curve matching method may not be able to resolve the different sea state levels across range. In these situations, the readers are referred to the techniques (described in [16], for example) that utilize the second-order sea clutter features in the Doppler spectrum.

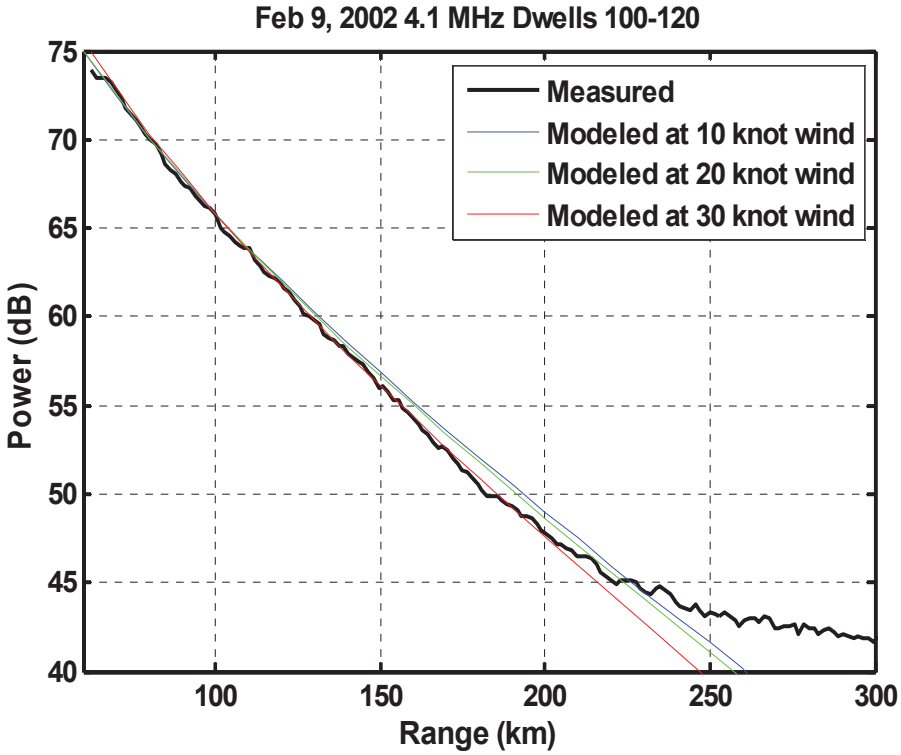

Figure 22 *Comparisons between modelled sea clutter attenuation curves for various sea states and the measured sea clutter attenuation at 4.1 MHz (sea state: High+).*

Table 6 Sea state matching with the HFSWR at 4.1 MHz

Wind Speed (knots)	Δ_{rms} (dB)
30	0.247
20	0.395
10	0.486

The discussion in this section above is intended to demonstrate in a different way the accuracy of the modelled ground-wave propagation attenuation over rough seas. The differences between the added losses in different sea states show that the ground-wave propagation attenuations in the lower sea states are inseparable, but the ground-wave propagation in the High+ sea state at the radar frequency of 4.1 MHz is separable from those in the lower sea states. The result in Figure 22 clearly demonstrates that the measured sea clutter attenuation in that High+ sea state at the radar frequency of 4.1 MHz can be used to resolve the modelled sea clutter attenuations in the three sea states, and therefore determines that sea state, on the basis of the assumption that the sea state is constant in range.

6.2 Detection of ionospheric distortions

Most theoretical HFSWR simulations are based on the assumption that the radar transmits and receives ground-wave signals only. In reality, the radar antennas are susceptible to not only surface wave, but also skywave, and the ground-wave radar signal can be distorted by skywave signal components such as ionospheric clutter and external interference, resulting in detection performance degradations.

In the first two sub-sections below, we show the sensitivities of the modelled sea clutter attenuation to either ionospheric clutter or skywave interference in the radar data measured from the selected steady sea states. In Section 6.2.3, we comment on the potential applications of the modelled sea clutter attenuation after the validation in coastal surveillance HFSWR.

6.2.1 Sensitivity to ionospheric clutter

Figure 19 has actually already shown how the validated ground-wave propagation attenuation can be used to detect even a minute amount of performance degradation caused by one of these skywave signal components. As indicated in Section 5.2.3, in the range interval between 100 and 160 km, the measured sea clutter attenuation was elevated slightly (2 dB max.) from the modelled sea clutter attenuation. This indicates that the HFSWR sea clutter was likely distorted by the ionospheric clutter from the E layer clutter, which was unexpected at night at the radar frequency of 4.1 MHz. An inspection of the clutter intensity map of the data collected for the day (similar to those shown in Figure 6) shows that there was indeed the presence of the E-layer clutter in the radar data, possibly due to the remnant effects of an earlier sporadic-E clutter storm.

6.2.2 Sensitivity to external interference

In reality, the ground-wave sea echo is actually superimposed on an apparent noise floor that could change with the level of external interference. To model the received radar signal, we must add this level of apparent noise to the ground-wave sea echo. The two sets of 4.1-MHz radar data used for the validation of the ground-wave propagation attenuation over High and High+ seas were measured during periods of time when the altitudes of the F layer were near the highest on two different days in January and February, respectively. During these periods of time, typically a couple of hours after the local midnight, the F layer could be as high as 400 km. The large separation in range between the sea clutter and F layer clutter allows for the estimation of the apparent noise level, on the assumption that the sea clutter and apparent noise are uncorrelated. Figures 23 and 24 show the range attenuation curves of the modelled radar signals for the two high sea states, respectively, together with those shown previously in Figures 17 and 18. One can observe from Figures 23 and 24 that the attenuation curves for the modelled and measured radar signals agree very well with each other. By comparing these latter two figures, however, one can notice that there is a difference in the apparent noise level. The apparent noise level in Figure 23 is about 4 dB higher than that in Figure 24. The original colour clutter-intensity maps show that the 4.1-MHz radar channel was clear on both days. However, this slightly elevated noise floor indicates that the data in Figure 23 might have been contaminated with low-level external interference. An adjustment of the clutter-intensity map to a different colour scale reveals that there was indeed the presence of low-level external interference, which was shown in the plot on the right-hand side of Figure 6. Further analysis of the radar data indicates that the low-level

external interference was due to a sidelobe response of the radar receive array to a dominant interferer.

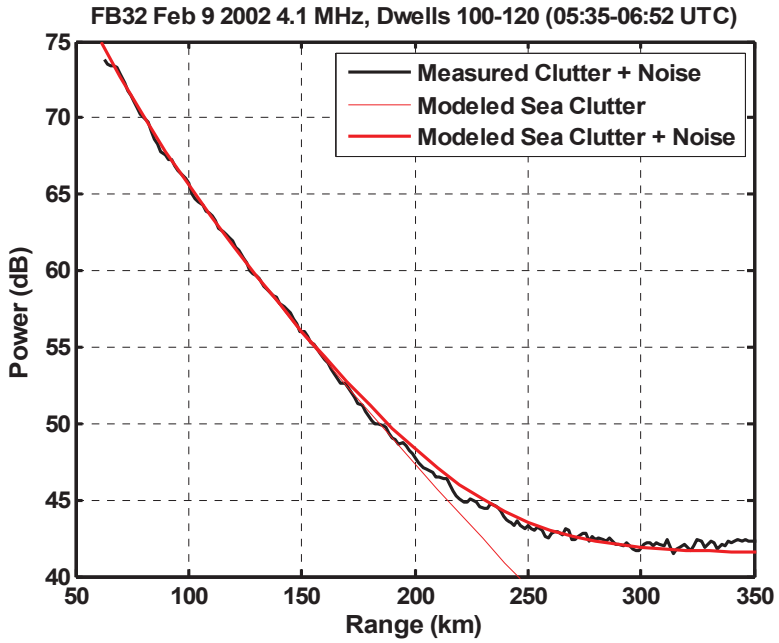

Figure 23 *Comparison between modelled and measured ground-wave radar signal attenuation (sea clutter + noise) at 4.1 MHz (sea state: High+).*

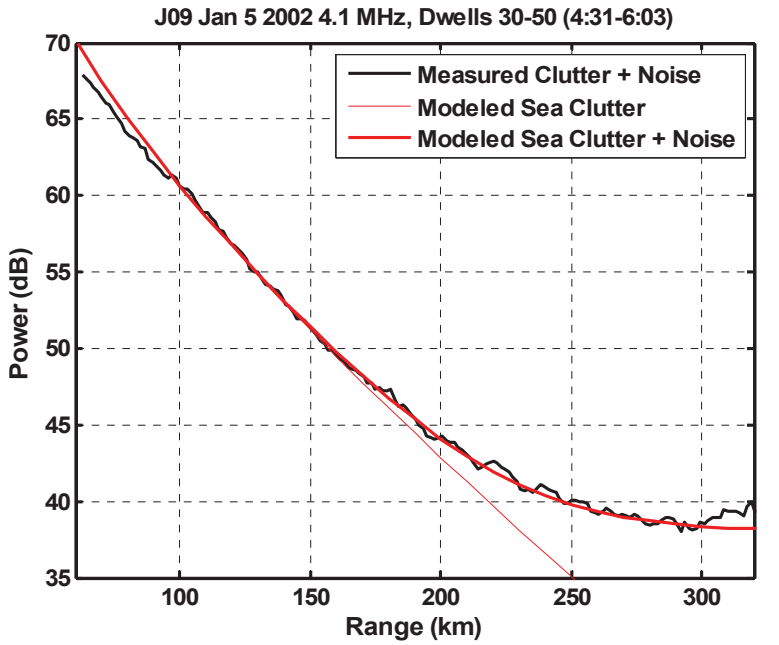

Figure 24 *Comparison between modelled and measured ground-wave radar signal attenuation (sea clutter + noise) at 4.1 MHz (sea state: High).*

6.2.3 Potential applications of the modelled sea clutter attenuation in coastal surveillance HFSWR

The two examples above show that the modelled sea clutter attenuation is highly sensitive to the presence of the skywave interference or ionospheric clutter when the sea state is relatively steady.

The skywave signal components are typically an order of magnitude larger than the modelled sea clutter level at the far side of the radar coverage. Hence, for the detection of the skywave signal components, the requirement on the fidelity of the modelled sea clutter attenuation is not as stringent as that for the validation of the ground-wave propagation attenuation. In addition, the duration over which the median sea clutter level is estimated can be shortened to accommodate the change of the sea state in the radar coverage. With the reasonable assumption that the sea state over the propagation path is constant over a shorter duration, it is expected that the modelled sea clutter attenuation can be used to detect the presence of the skywave signal components in any observable sea states.

The attenuation of the clutter between the Bragg lines can thus be used together with the measured external noise level to establish a baseline for the ground-wave radar signal attenuation. This baseline could be either theoretical or measured – it is theoretical if the modelled sea clutter attenuation is used, but it is measured if the attenuation of the measured clutter level between the Bragg lines is used. Potential applications of the theoretical and measured baselines include:

1. Generation of a simple, yet reliable, clutter map that meets the operation requirement by indicating the expected levels of radar performance for different targets of interest. The signals of the targets can be measured at a close range and the attenuations of the target signals can be calculated by using the validated ground-wave propagation attenuation. The clutter map can then be generated by comparing the modelled target signal attenuations with the attenuations of the measured clutter-plus-interference-and-noise levels from all azimuthal beam directions.

2. The ground-wave radar signal attenuation baseline can also be used to facilitate optimal implementations of various signal processing algorithms in the radar receiver, and therefore potentially improve the radar performance. In [17], for example, we have used the baseline to identify the region of dominance by skywave interference and revised the existing interference suppression algorithm to significantly improve its performance. Note that the duration to estimate the median clutter level was reduced to 5 dwells only in the cases of high sea states in [17].

3. Better identification of the different regions of dominance by the different HFSWR signal components may also enable better selections of optimal detectors for the different regions. As demonstrated in [18], this has the potential to improve the detection performance of the radar. The ground-wave radar signal attenuation baseline provides a simple but effective means to identify these different regions.

4. As mentioned in Section 2.4, the ground-wave radar signal attenuation baseline can also be used to greatly facilitate the assessment of the radar performance, which is expected for the development of any new radar. This baseline can be used to detect the presence of

skywave interference and ionospheric clutter, as well as to quantify the subsequent performance degradations of the radar.

7. Conclusions and recommendations

The report set out to investigate whether it would be feasible to use the second-order sea clutter continuum between the Bragg lines to validate the modelled ground-wave propagation attenuation over a rough sea. The conclusion is that the modelled data are validated statistically.

A homogeneous propagation medium is assumed in the model of the ground-wave propagation attenuation. This requires the sea state to be steady in time and constant across range. Ideally, the conditions of a fully developed sea would meet this requirement. However, in reality, the conditions of a fully developed sea are unattainable. Hence, we used a less restrictive but more practical approach to select the sea-clutter data from the non-interfered nighttime HFSWR data. In this data-selection approach, the sea state level in the region of interest was roughly indicated by the significant wave height readings from the wave buoy at the far side of the radar coverage, and the steadiness of the sea state at a close range in the region was closely monitored by the variation of the median sea clutter level from that range itself. The feasibility of the validation was then tested over the range interval where the second-order sea clutter continuum was dominant. A total of eight sets of HFSWR data were selected, respectively, representing cases in four different levels of sea states at two radar frequencies between 3 and 5 MHz.

The results show that the measured and modelled sea clutter attenuations agree very well in all the cases. In general, the higher the sea state, the better the agreement, likely because the conditions of the higher sea states resembled better those of a fully developed sea.

The effectiveness of the validation using a dedicated ship target was then compared with that of the validation using the second-order sea clutter. It is shown that the validation approach using the second-order sea clutter is far more effective than that using the dedicated target signal. The results also show that the median of the averaged sea clutter continuum is actually a more stable radar echo than the dedicated target signal for the validation.

The report then investigated the possibility of determining the sea state in the radar coverage by comparing the measured sea clutter attenuation with the sea clutter attenuations modelled for a number of sea states with the commonly observed wind speeds. It is found that the measured sea clutter attenuation can be used to match with the modelled sea clutter attenuation to determine the steady high sea states when the radar operates at or above the frequency of 4.1 MHz based on the assumption that the sea state is constant in range. This ability of the measured sea clutter attenuation to resolve the modelled sea clutter attenuations is another way to demonstrate the accuracy of the modelled ground-wave propagation attenuation.

With the ground-wave propagation attenuation validated, the report then examined the sensitivity of the modelled sea clutter attenuation to ionospheric clutter and skywave interference. It is found that the modelled sea clutter attenuation is highly sensitive to each of the skywave signal components in the radar data that were measured in relatively steady sea states. With the reasonable assumption that the sea state over the propagation path is constant, it is proposed that the modelled sea clutter attenuation be used to establish a baseline in a HFSWR system for the detection of ionospheric clutter and skywave interference. The potential applications of this ground-wave radar signal attenuation baseline include a simple yet highly reliable clutter map, optimized implementations of certain modules in the received radar signal processing chain, and

assessments of the degradations from theoretically simulated HFSWR performance, as discussed in Section 6.2.3 of this report.

During the course of the current investigation, several unusual forms of ionospheric clutter were also observed. It is recommended that the validated ground-wave propagation attenuation be used to further study, and possibly uncover more of, the distortion behaviours of the various forms of ionospheric clutter, including those of the mixed-path. It should be noted that these various forms of ionospheric clutter could also be observed from the Doppler spectra, but their impact on the radar performance might not have been fully assessed.

References

[1] Barrick, D. E. (1971), “Theory of HF and VHF propagation across the rough sea, Parts 1 and 2”, Radio Science, 6, pp. 517-533.

[2] Hill, R. S. (1985), "Ground-wave propagation program GRWAVE", MTR 85/45, Marconi Research Centre, U.K.

[3] Leong, H. and Wilson, H. (2006), “An estimation and verification of vessel radar cross sections for HF surface wave radar”, IEEE Antennas and Propagation Magazine, Vol. 48, No. 2, April, pp. 11-16.

[4] Leong, H. (2007), “An estimation of radar cross sections of small vessels at HF”, IET International Radar Conference (RADAR 2007), Edinburgh, Scotland, October 15-18.

[5] Leong, H. (2002), “Dependence of HF-surface-wave-radar sea clutter on sea state”, IEE International Radar Conference (RADAR 2002), Edinburgh, Scotland, October 15-17, pp. 56-60.

[6] Leong, H. and Ponsford, A. (2008), “The Effects of sea clutter on the performance of HF surface wave radar in ship detection”, IEEE National Radar Conference (RadarCon 2008), Rome, Italy, May.

[7] Leong, H., Dawe, B. and Power, D. (2000), “Noise measurements at Cape Race in support of East-Coast High Frequency surface wave radar”, DREO TM 2000-089.

[8] Larsen, R. and Pielou, J. M. (1989), “An HF oversea ground-wave path loss experiment”, Proceedings of IEE Sixth International Conference on Antenna and Propagation (ICAP89), Conventry, UK, April 4-7.

[9] Pielou, J. M. and Larsen, R. (1990), “HF ground-wave oversea path loss prediction”, IEE Colloquium on “The interaction of radiowave with the sea surface” (Digest No. 037), London, UK, February 21.

[10] Barrick, D. E. (1972), “Remote sensing of sea state by radar”, in "Remote Sensing of Troposphere", Edited by V. E. Derr, GPO, Washington, DC.

[11] Hasselmann, K. (1971), “Determination of ocean wave spectra from Doppler radio return from the sea surface”, Nature Phys. Sci., 229, 16-17.

[12] Wilson, H. and Leong, H. (2003), “A technical evaluation of the High Frequency surface wave radar at Cape Race, Newfoundland”, DRDC Ottawa TR 2003-013, January.

[13] Milsom, J.D. (1997), “HF groundwave radar equations”, Proc. of HF Radio Systems and Techniques, July 7-11, UK.

[14] Phillips, O. M. (1977), “The Dynamics of the upper ocean”, 2nd Ed., Cambridge University Press.

[15] http://www.meds-sdmm.dfo-mpo.gc.ca/isdm-gdsi/waves-vagues/overview-apercu-eng.html

[16] Shearman, E. D. R. (1981), “Remote sensing of ocean wavs, currents and surfaces winds by dekametric radar”, in “Remote sensing in meteorology, oceanography and hydrology”, Edited by Cracknell, A. P., Ellis Horwood Ltd.

[17] Leong, H. (2011), “Improved detection and suppression of skywave interference in HFSWR”, International Radar Symposium (IRS-2011), Leipzig, Germany, September.

[18] Wang, E., Wang, J. and Ponsford, A. (2011), “An adaptive hierarchal CFAR for optimal target detection in mixed clutter environments”, IEEE Radar Conference (RadarCon 2011), Kansas City, USA, May.

Appendix A Basic transmission losses

Barrick's BTL, as presented in [1], has a lower bound of $(2\pi R/\lambda)^2$, where λ is the radar wavelength, and is related to Grwave's BTL (L_b) by

$$L_b = L_{Bar} r_t r_r , \tag{A-1}$$

where r_t and r_r are the ratios of the radiation resistances of the transmit and receive antennas when positioned at certain heights (h_t and h_r) above a perfectly conducting ground plane to those in free space, respectively (refs. Appendix C of [2] and [13]). These are often referred to as the height factors as they relate the effects of the couplings between the antennas and the ground plane to the antenna heights. Grwave models r_t and r_r by using the height factor theoretically derived for a small dipole above a perfectly conducting plane. For vertical polarization, the height factor for the small dipole varies between 1 and 2. When the antenna is at more than one wavelength above the ground, the height factor is close to be 1, and L_b and L_{Bar} are approximately equal with a lower bound prescribed by $(2\pi R/\lambda)^2$. When the antenna is on the ground, e.g., a monopole mounted on top of a perfectly conducting ground, the height factor is equal to 2, and L_b is about 6 dB greater than L_{Bar}. In this latter case, Grwave's BTL (L_b) has a lower bound that is equal to the one-way free-space transmission loss value of $(4\pi R/\lambda)^2$.

The fact that L_b and L_{Bar} in the former case have a lower bound of $(2\pi R/\lambda)^2$, rather than $(4\pi R/\lambda)^2$, indicates that both Barrick and Grwave have included the effect of ground reflection in the basic transmission losses. Grwave's BTL would decrease by 3 dB when one of the two antennas is elevated from the ground to a height above one wavelength, and by 6 dB when both the antennas are elevated. However, very little change with antenna heights can be observed in Barrick's BTL when the separation between the two antennas is much greater than the antenna heights (i.e., the small change in the antenna height does not have much impact on the separation). Hence, Barrick's BTL does not include the effect of mutual coupling between the antennas and the conductive ground plane (the so-called ground proximity effect), whereas Grwave's BTL includes this effect.

As mentioned in the introductory chapter, we have used Barrick's modified surface impedance in Grwave to calculate the ground-wave propagation attenuation. In order to match the calculated propagation attenuation with Barrick's BTL, we have removed the height factors in Grwave from the calculation. This modelled BTL is simply referred here to as the ground-wave propagation attenuation.

Appendix B Measured significant wave heights

The two wave buoys, each located at Nickerson Bank and the Tail of the Bank, were set up to provide hourly measurements of the ocean wave spectra and wind velocities at the two locations. Figure B-1 shows the significant wave heights measured from the two wave buoys for the selected periods between January and August, 2002 in which data from the radar at Cape Race were also measured. There were a total of 15 selected periods for the wave buoy data, and the durations of these periods ranged from one to seven days. Note that the significant wave heights are shown in time, relative to 00:00 on the first day of each period.

Figure B-1 shows that, the variation trends of the significant wave heights from the two wave buoys generally agree well with each other, but the significant wave height measured from the Tail of the Bank is mostly higher than that measured from Nickerson Bank, particularly during periods of high sea states (e.g., Jan 25-29 and Feb 8-9, 2002), likely because the wave buoy at Nickerson Bank is closer to the shoreline.

The measurements from the two wave buoys were mostly continuous, but occasionally there were interruptions. For example, the wave height measurements from Nickerson Bank were quite intermittent during the period of February 8 and 9, 2002. For 17 hours between 17:00 on February 8 and 09:00 on February 9, 2002, there were only two outputs of the significant wave height, instead of the expected hourly measurements (ref to the third plot in Figure B-1).

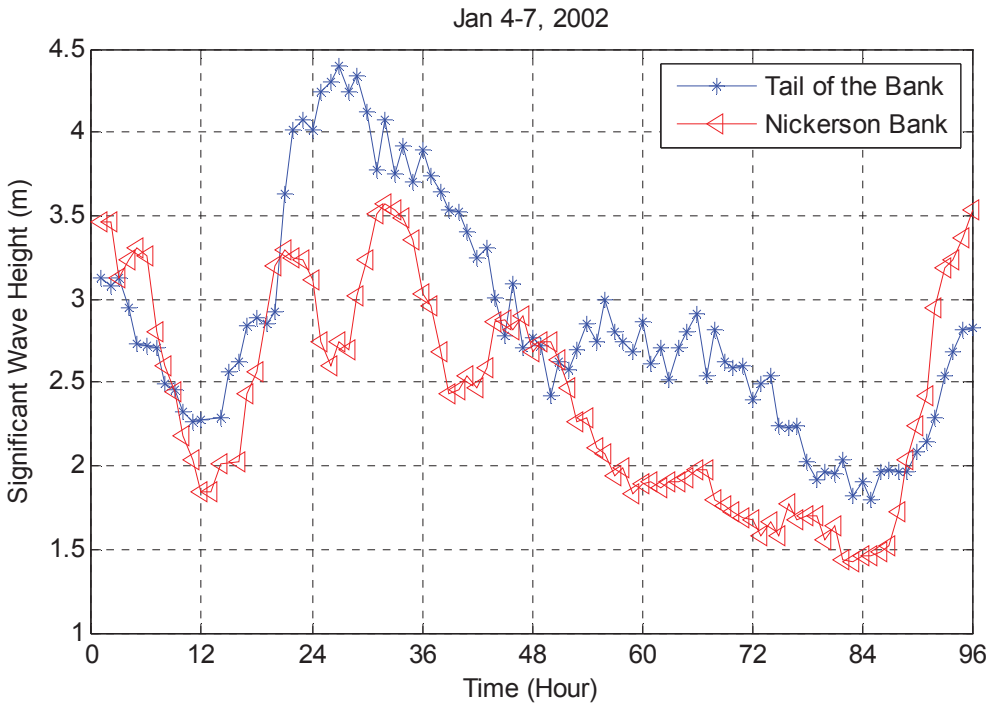
Jan 4-7, 2002
Tail of the Bank
Nickerson Bank
Significant Wave Height (m)
Time (Hour)
4.5
4
3.5
3
2.5
2
1.5
1
0
12
24
36
48
60
72
84
96

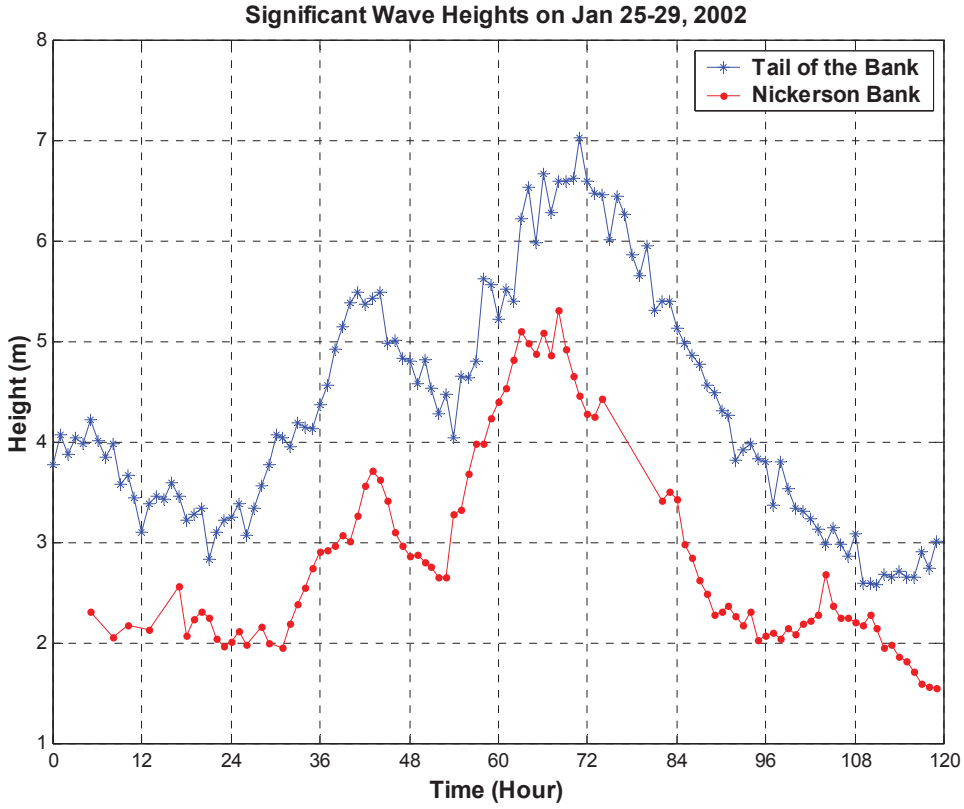
Significant Wave Heights on Jan 25-29, 2002
Tail of the Bank
Nickerson Bank
Height (m)
Time (Hour)
8
7
6
5
4
3
2
1
0
12
24
36
48
60
72
84
96
108
120

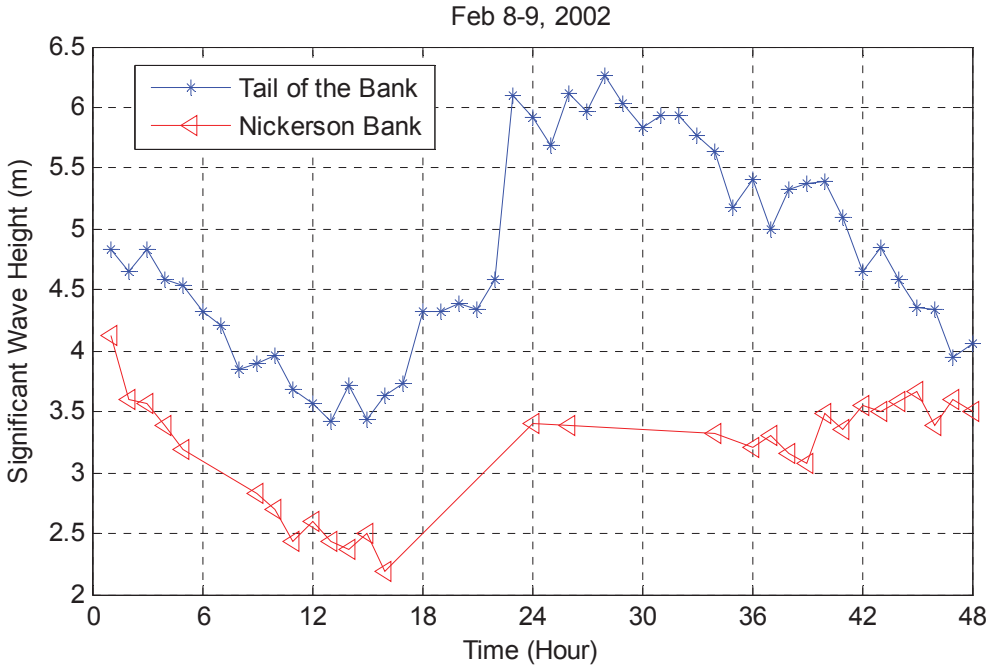
Feb 8-9, 2002
Tail of the Bank
Nickerson Bank
Significant Wave Height (m)
Time (Hour)
6.5
6
5.5
5
4.5
4
3.5
3
2.5
2
0
6
12
18
24
30
36
42
48

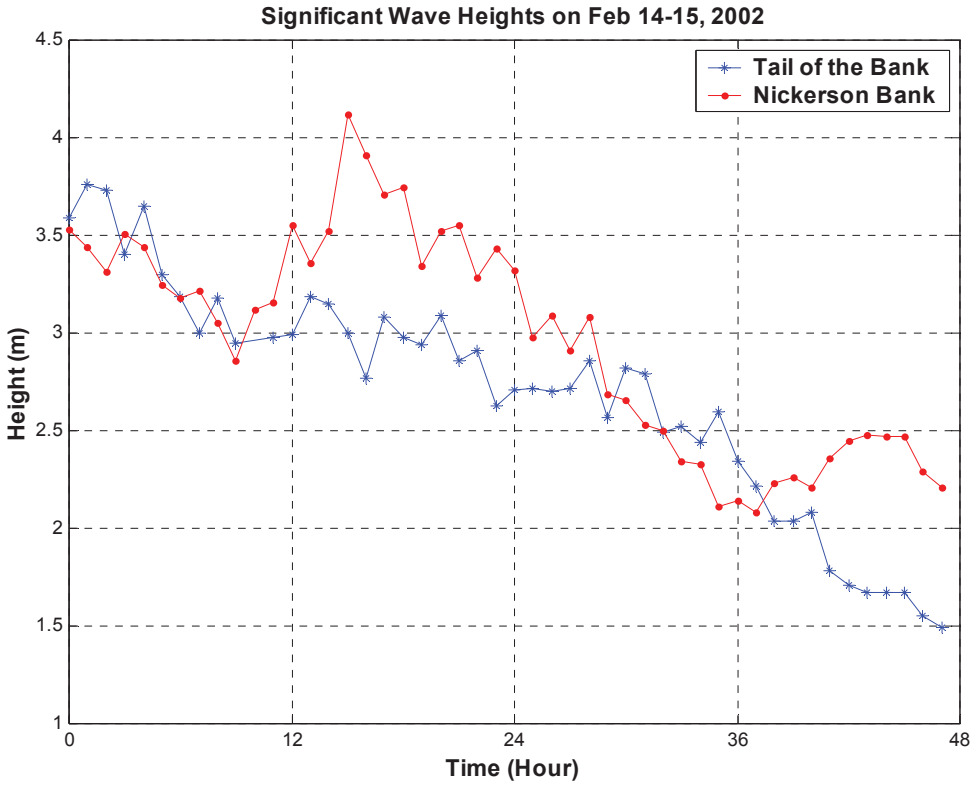
Significant Wave Heights on Feb 14-15, 2002
Tail of the Bank
Nickerson Bank
Height (m)
Time (Hour)
4.5
4
3.5
3
2.5
2
1.5
1
0
12
24
36
48

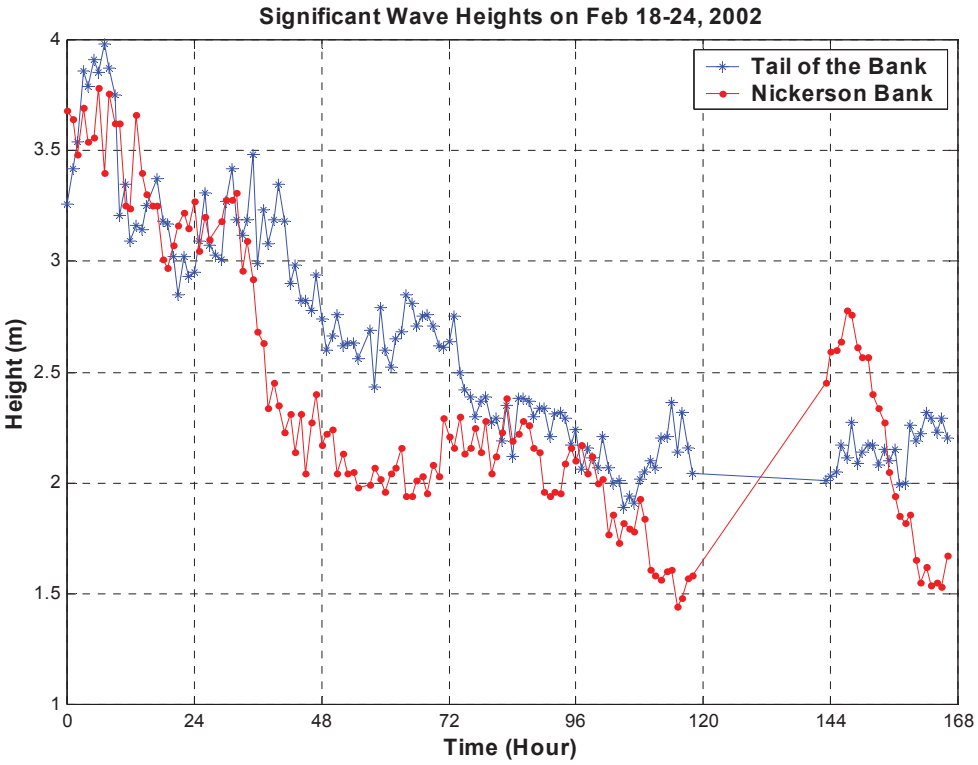
Significant Wave Heights on Feb 18-24, 2002
Tail of the Bank
Nickerson Bank
Height (m)
Time (Hour)
4
3.5
3
2.5
2
1.5
1
0
24
48
72
96
120
144
168

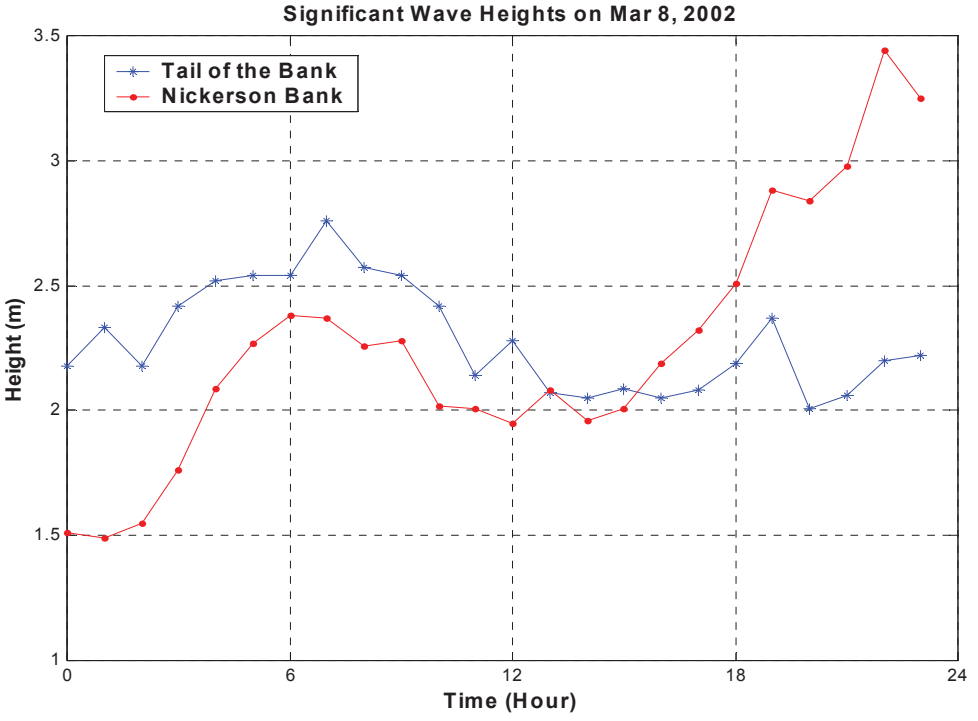
Significant Wave Heights on Mar 8, 2002
Tail of the Bank
Nickerson Bank
Height (m)
Time (Hour)
3.5
3
2.5
2
1.5
1
0
6
12
18
24

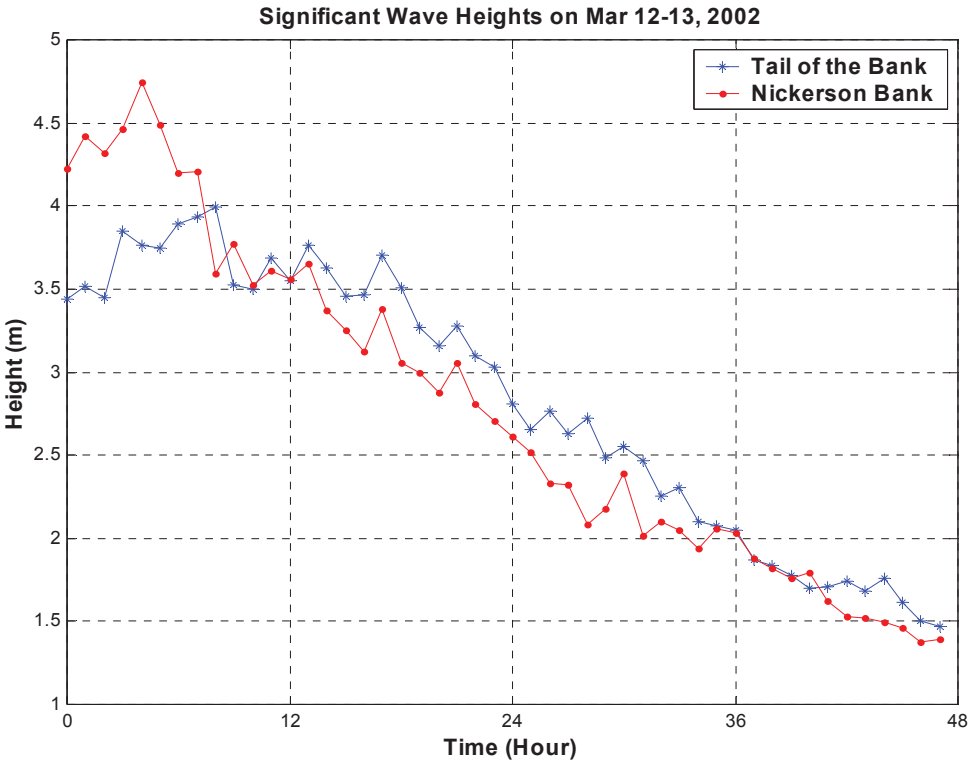
Significant Wave Heights on Mar 12-13, 2002
Tail of the Bank
Nickerson Bank
Height (m)
Time (Hour)
5
4.5
4
3.5
3
2.5
2
1.5
1
0
12
24
36
48

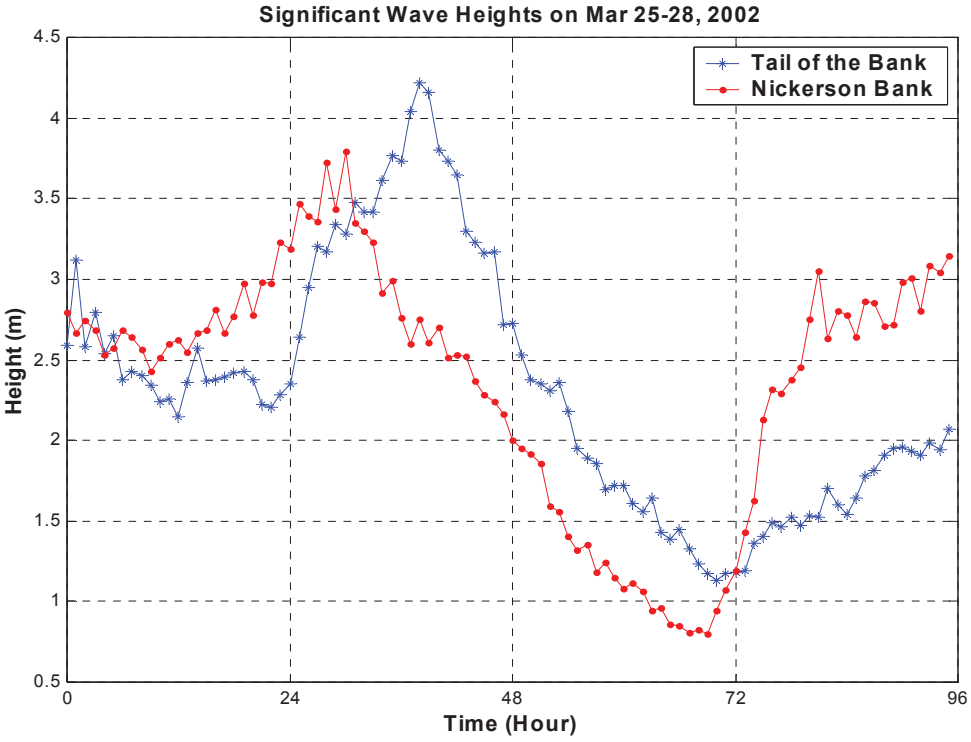
Significant Wave Heights on Mar 25-28, 2002
Tail of the Bank
Nickerson Bank
Height (m)
Time (Hour)
4.5
4
3.5
3
2.5
2
1.5
1
0.5
0
24
48
72
96

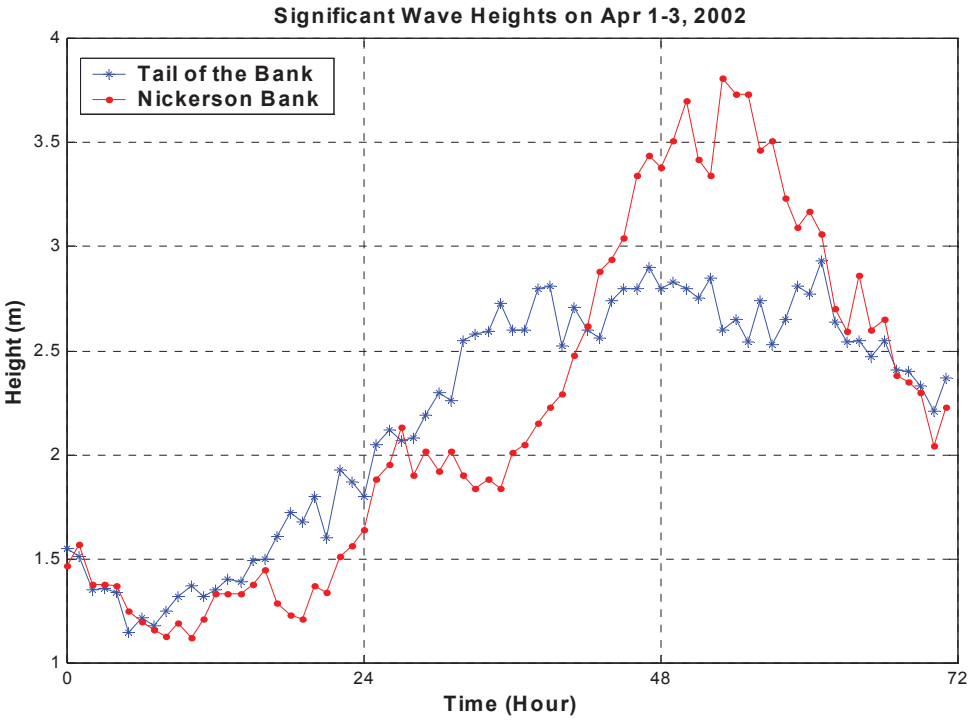
Significant Wave Heights on Apr 1-3, 2002
Tail of the Bank
Nickerson Bank
Height (m)
Time (Hour)
4
3.5
3
2.5
2
1.5
1
0
24
48
72

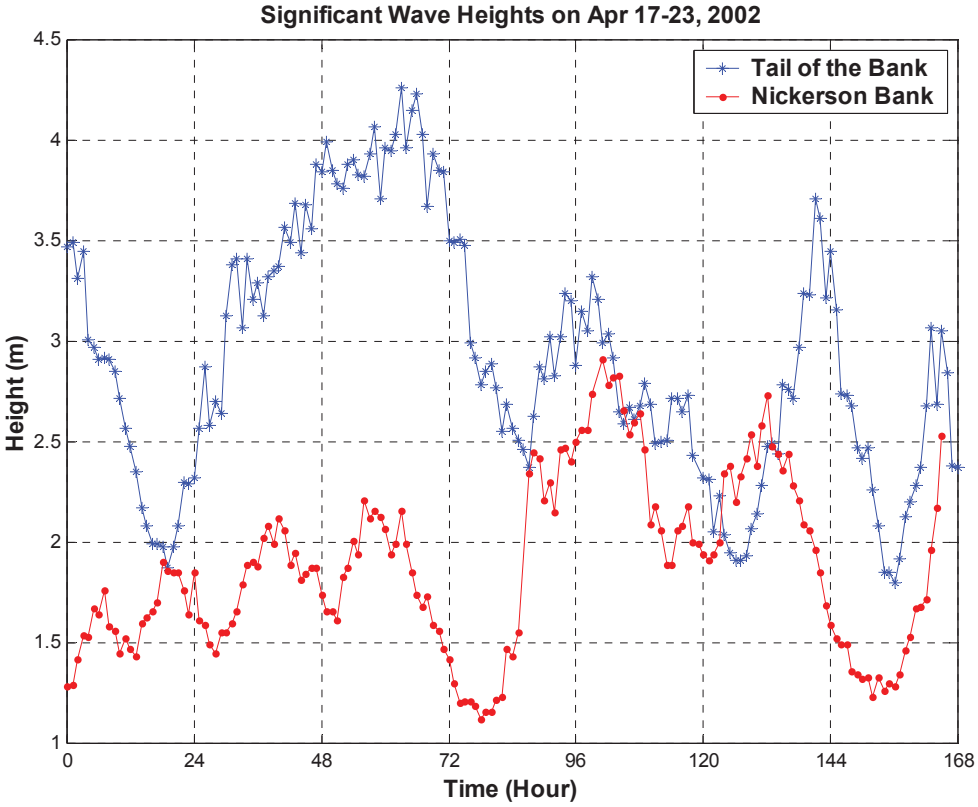
Significant Wave Heights on Apr 17-23, 2002
Tail of the Bank
Nickerson Bank
Height (m)
Time (Hour)
4.5
4
3.5
3
2.5
2
1.5
1
0
24
48
72
96
120
144
168

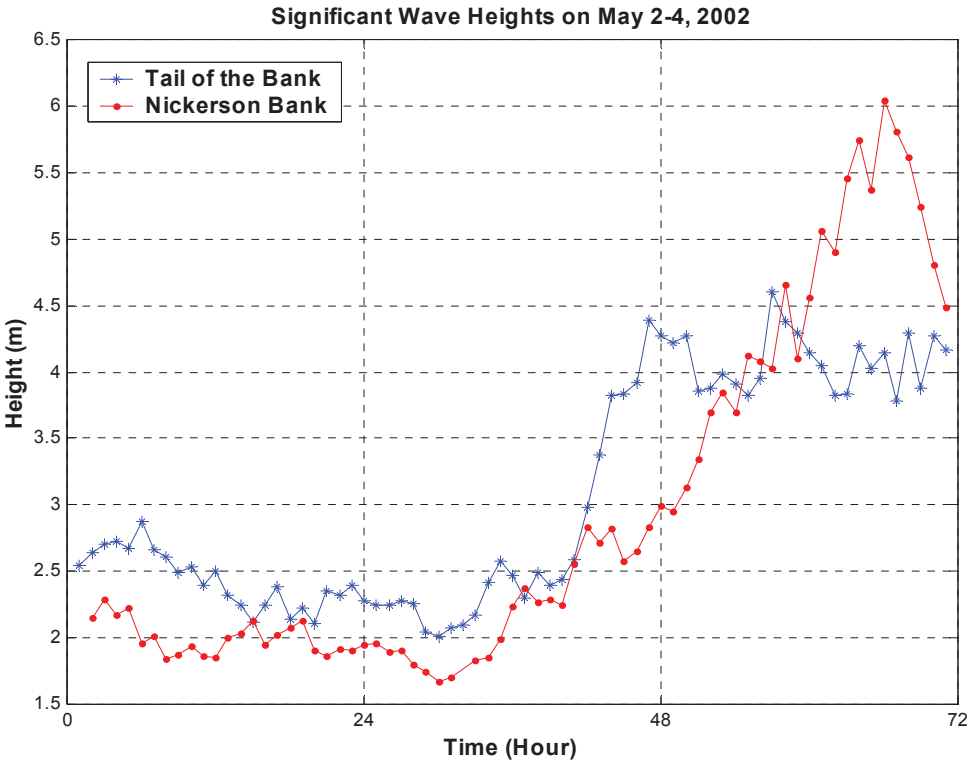
Significant Wave Heights on May 2-4, 2002
Tail of the Bank
Nickerson Bank
Height (m)
Time (Hour)
6.5
6
5.5
5
4.5
4
3.5
3
2.5
2
1.5
0
24
48
72

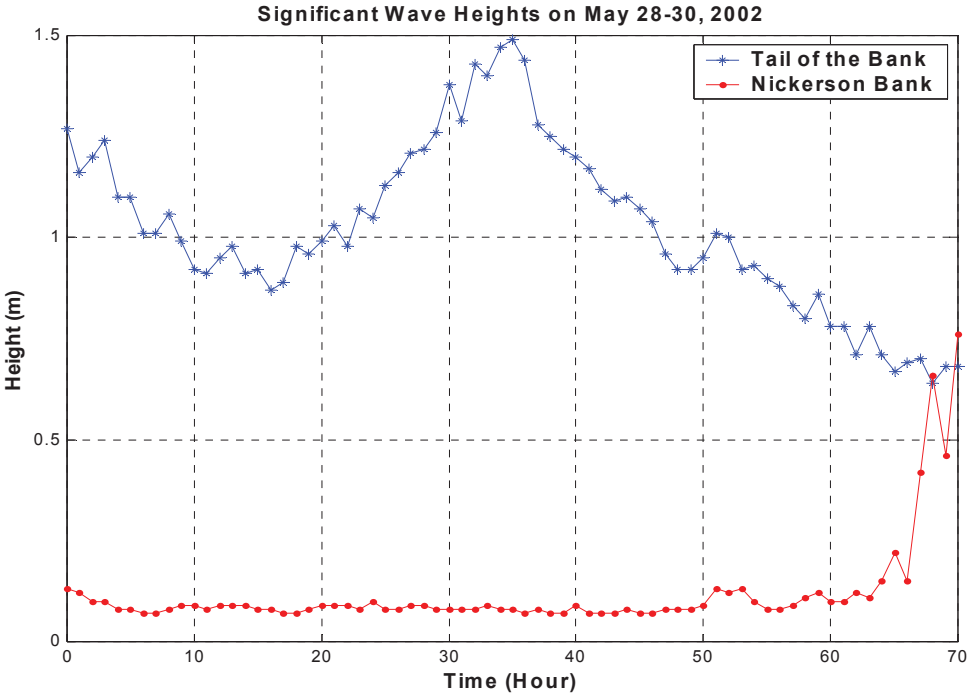
Significant Wave Heights on May 28-30, 2002
Tail of the Bank
Nickerson Bank
Height (m)
Time (Hour)
1.5
1
0.5
0
0
10
20
30
40
50
60
70

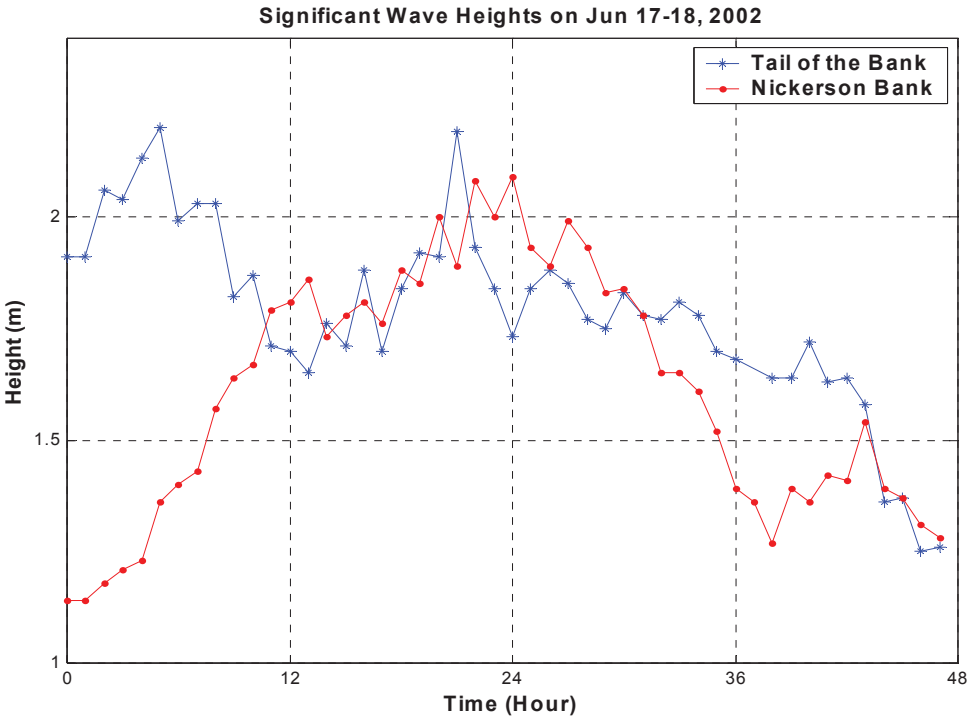
Significant Wave Heights on Jun 17-18, 2002
Tail of the Bank
Nickerson Bank
Height (m)
Time (Hour)
1
1.5
2
0
12
24
36
48

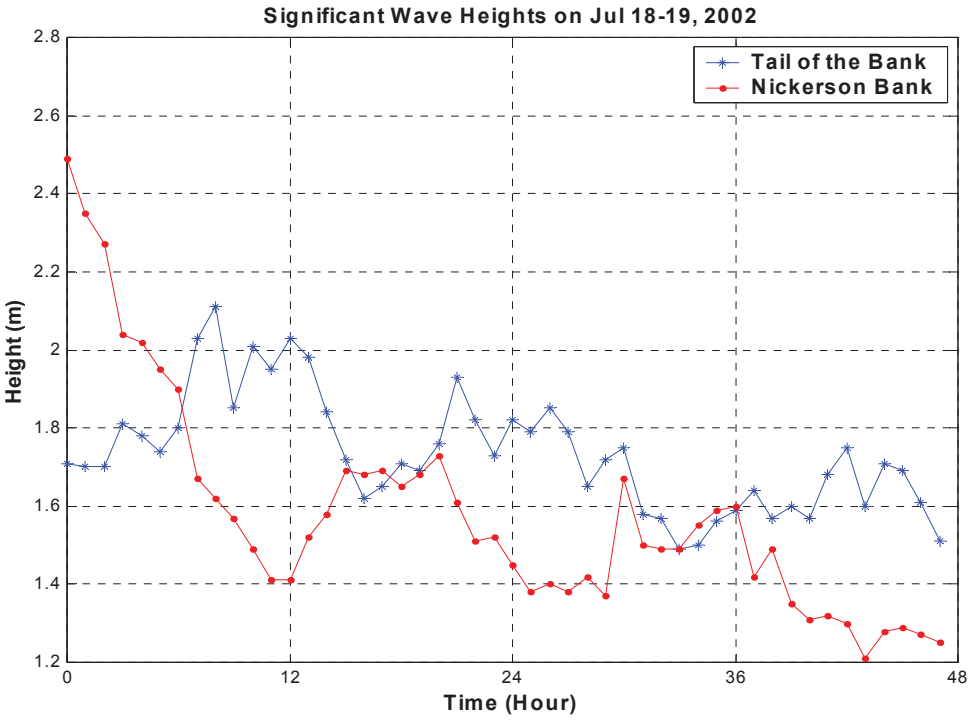
Significant Wave Heights on Jul 18-19, 2002
Tail of the Bank
Nickerson Bank
Height (m)
Time (Hour)
1.2
1.4
1.6
1.8
2
2.2
2.4
2.6
2.8
0
12
24
36
48

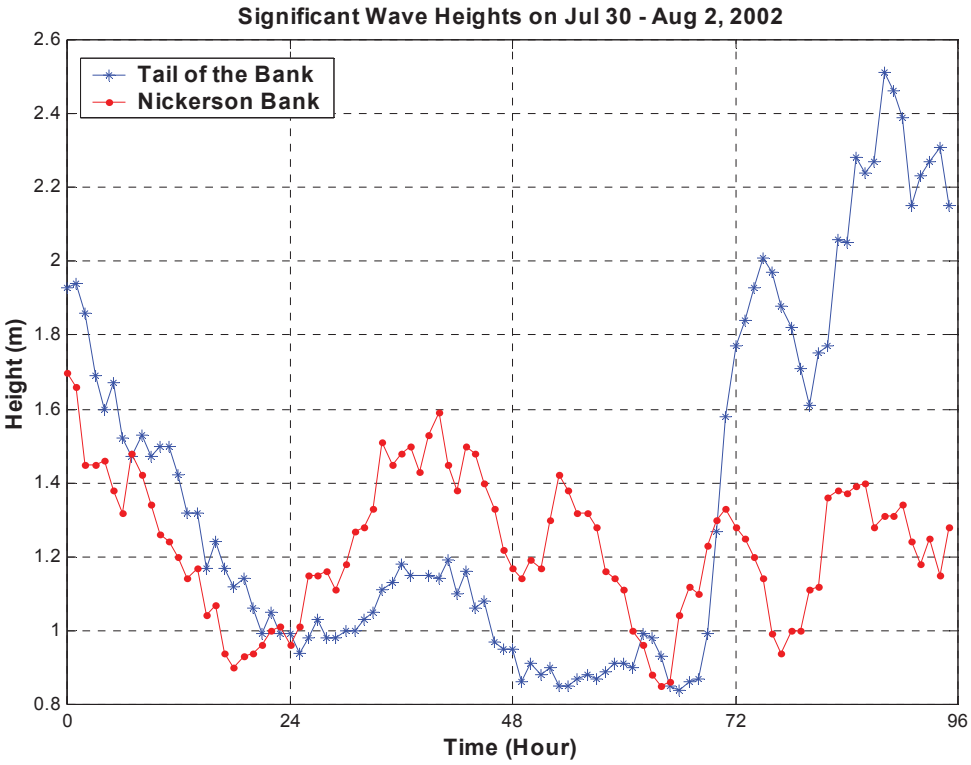

Figure B-1 *Significant wave heights measured from the Tail of the Bank and Nickerson Bank for 15 selected periods from January to August, 2002.*

DOCUMENT CONTROL DATA

(Security classification of title, body of abstract and indexing annotation must be entered when the overall document is classified)

1. ORIGINATOR (The name and address of the organization preparing the document. Organizations for whom the document was prepared, e.g. Centre sponsoring a contractor's report, or tasking agency, are entered in section 8.)

Defence R&D Canada – Ottawa
3701 Carling Avenue
Ottawa, Ontario K1A 0Z4

2. SECURITY CLASSIFICATION (Overall security classification of the document including special warning terms if applicable.)

UNCLASSIFIED
(NON-CONTROLLED GOODS)
DMC A
REVIEW: GCEC June 2010

3. TITLE (The complete document title as indicated on the title page. Its classification should be indicated by the appropriate abbreviation (S, C or U) in parentheses after the title.)

On the feasibility of using measured sea clutter continuum in HFSWR to validate modelled ground-wave propagation attenuation in rough sea

4. AUTHORS (last name, followed by initials – ranks, titles, etc. not to be used)

Leong, H.

5. DATE OF PUBLICATION (Month and year of publication of document.)	6a. NO. OF PAGES (Total containing information, including Annexes, Appendices, etc.)	6b. NO. OF REFS (Total cited in document.)
September 2012	70	18

7. DESCRIPTIVE NOTES (The category of the document, e.g. technical report, technical note or memorandum. If appropriate, enter the type of report, e.g. interim, progress, summary, annual or final. Give the inclusive dates when a specific reporting period is covered.)

Technical Report

8. SPONSORING ACTIVITY (The name of the department project office or laboratory sponsoring the research and development – include address.)

Defence R&D Canada – Ottawa
3701 Carling Avenue
Ottawa, Ontario K1A 0Z4

9a. PROJECT OR GRANT NO. (If appropriate, the applicable research and development project or grant number under which the document was written. Please specify whether project or grant.)	9b. CONTRACT NO. (If appropriate, the applicable number under which the document was written.)
11HJ	

10a. ORIGINATOR'S DOCUMENT NUMBER (The official document number by which the document is identified by the originating activity. This number must be unique to this document.)	10b. OTHER DOCUMENT NO(s). (Any other numbers which may be assigned this document either by the originator or by the sponsor.)
DRDC Ottawa TR 2012-015	

11. DOCUMENT AVAILABILITY (Any limitations on further dissemination of the document, other than those imposed by security classification.)

UNLIMITED

12. DOCUMENT ANNOUNCEMENT (Any limitation to the bibliographic announcement of this document. This will normally correspond to the Document Availability (11). However, where further distribution (beyond the audience specified in (11) is possible, a wider announcement audience may be selected.))

UNLIMITED

13. ABSTRACT (A brief and factual summary of the document. It may also appear elsewhere in the body of the document itself. It is highly desirable that the abstract of classified documents be unclassified. Each paragraph of the abstract shall begin with an indication of the security classification of the information in the paragraph (unless the document itself is unclassified) represented as (S), (C), (R), or (U). It is not necessary to include here abstracts in both official languages unless the text is bilingual.)

This report presents the results of an investigation on the feasibility of using the sea clutter continuum between the Bragg lines of monostatic HF Surface Wave Radar (HFSWR) to validate the ground-wave propagation attenuation model for rough sea, based on Barrick's formulation. The proposed validation is based on a comparison between the measured and modelled sea clutter levels from a variety of sea states over a range interval approximately between 63 and 200 km. The sea state in the interval was roughly indicated by the significant wave height measured at the far side of the radar coverage. The measured sea clutter is estimated from the median of the averaged power levels between the Bragg lines over a selected number of radar dwells in a moving window. The modelled sea clutter attenuation is then obtained by calibrating the modelled ground-wave propagation attenuation to the median sea clutter from a selected range bin in the near side of the chosen interval. The steadiness of the sea state in the selected range bin was closely monitored by the variation of the median from that range. If this median is deemed to be steady over the duration of the moving window, then the radar data segment is chosen for the investigation. The results show that the measured and modelled sea clutter attenuations agree well over the chosen interval in four different sea states at two radar frequencies. The validation is also compared with that using a dedicated ship target. It is found that the median sea echo was actually more stable than the target signal for the validation. Furthermore, the modelled sea clutter attenuation is shown to be highly sensitive to the presence of either ionospheric clutter or skywave interference. With a reasonable assumption that the sea state over the propagation path is constant, the modelled sea clutter attenuation after the validation can be used in high confidence to detect the skywave signal components.

14. KEYWORDS, DESCRIPTORS or IDENTIFIERS (Technically meaningful terms or short phrases that characterize a document and could be helpful in cataloguing the document. They should be selected so that no security classification is required. Identifiers, such as equipment model designation, trade name, military project code name, geographic location may also be included. If possible keywords should be selected from a published thesaurus, e.g. Thesaurus of Engineering and Scientific Terms (TEST) and that thesaurus identified. If it is not possible to select indexing terms which are Unclassified, the classification of each should be indicated as with the title.)

High Frequency Surface Wave Radar, HFSWR, ground-wave propagation attenuation over rough sea, coastal surveillance, ship detection, sea clutter, sea state.

Defence R&D Canada

Canada's leader in Defence
and National Security
Science and Technology

R & D pour la défense Canada

Chef de file au Canada en matière
de science et de technologie pour
la défense et la sécurité nationale

DEFENCE DÉFENSE

www.drdc-rddc.gc.ca